ET Portioning using isotopes

STUDY TEAM

Sr. No.	NIH, Roorkee	IIT-Kanpur
1	Dr. Gopal Krishan, Scientist-E and Principal Investigator, HID	Prof. Shivam Tripathi, Principal Investigator, Dept Civil Engineering
2	Dr. M.S. Rao, Scientist-G, HID	Prof. Richa Ojha, Dept Civil Engineering
3		Prof. Rajesh Srivastava, Dept Civil Engineering
4		Prof. Saumyen Guha, Dept Civil Engineering

Submitted to
DST-SERB

Jointly Submitted by

	National Institute of Hydrology, Roorkee-247 667		**Indian Institute of Technology, Kanpur**

March, 2025

Technical Report

I. Concise Research Accomplishment

1. **Establishment of field experimental sites:** Two sites, one inside IIT Kanpur and the other 15 km north of IIT Kanpur at Bithoor, are established.

2. **Design, construction and installation of instruments**: Many instruments required in the project were either not commercially available or too expensive to be viable for research purposes. These instruments were designed, tested and fabricated in-house. Some examples are:
   a) Mini-lysimeters with automatic weighing system and facilities for data logging and transmission over Wi-Fi.
   b) An automatic rainwater sampling system for collecting rainwater samples at user-defined intervals.
   c) A liquid nitrogen trap-based air intake structure for collecting atmospheric water vapour samples simultaneously at multiple heights.
   d) An evaporation chamber for capturing water evaporating from bare soils.

3. **Data collection:**
   a) Hydrometeorological data at 15 minutes intervals for variables including rainfall, soil moisture, wind, temperature, humidity, short-and long-wave radiation and soil-heat flux.
   b) Crop data measured weekly consisted of plant height, root depth, leaf area index and above-ground biomass.
   c) Samples for isotope analysis: Soil samples at multiple depths, plant leaf and stem samples at multiple locations, all rain events, irrigation, river water, atmospheric water and dewater at the two experimental sites in Kanpur. Further, samples for soil evaporation, plant transpiration and groundwater were collected at NIH Roorkee.

4. **Standardization and establishment of protocols for isotope analysis:** The procedure for extracting soil, plants and atmospheric water were standardized. The analytical precision of the isotope analyzer was quantified and the procedure for optimally analyzing samples was fixed.

5. **Data Analysis and evapotranspiration partitioning:** A local meteoric water line is developed. The collected water samples were analyzed to partition evapotranspiration into evaporation and transpiration components. The results of the isotopic method were compared with the hydrometric method. The transpiration fraction in evapotranspiration (T/ET) was measured to be in the range of 0.45 to 0.60 for wheat season with significant inter- and intra-seasonal variability. The measured T fraction of ET was comparatively lower than that reported for irrigated wheat crops from other parts of the world (0.44 to 0.76) indicating low irrigation efficiency in the study area. Experiments carried out at NIH Roorkee showed that the process of evaporation from the soil surface during the post-monsoon period progresses in parallel with other hydrological processes, such as capillary action and diffusion-driven downward flux of enriched water molecules. This results in the broadening of an isotopically enriched layer of soil moisture in the

vadose zone with time. The plants and trees transpire this enriched water into the atmosphere, enriching it with heavy isotopic composition compared to the monsoon period.

II. Experimental/ Theoretical Investigation carried out

The experimental investigations carried out at IIT Kanpur and NIH Roorkee are described below. Tables and figures not included in the main report are provided at the end of this document and referred to here as Appendix information with prefix "A".

IIT Kanpur

1. **Experimental sites:** The two study sites selected for the project are shown in *Figure 1*. The sites are in the upper Gangetic plains of Uttar Pradesh where rice-wheat cropping system is widely practiced. The study area receives 815.9 mm of annual rainfall, with an average of 41.4 rainy days (1991-2020). Most of the rainfall occurs during June to September when the southwest monsoon is active in the region. The potential evapotranspiration (1090.5 mm/year) exceeds the annual rainfall. Both experimental sites have silty loam soil texture, with silt as the dominant fraction (*Table A1*). The IIT Kapur site has a slightly higher silt content (78.49–81.11%) compared to the Bithoor site (76.1–77.4%).

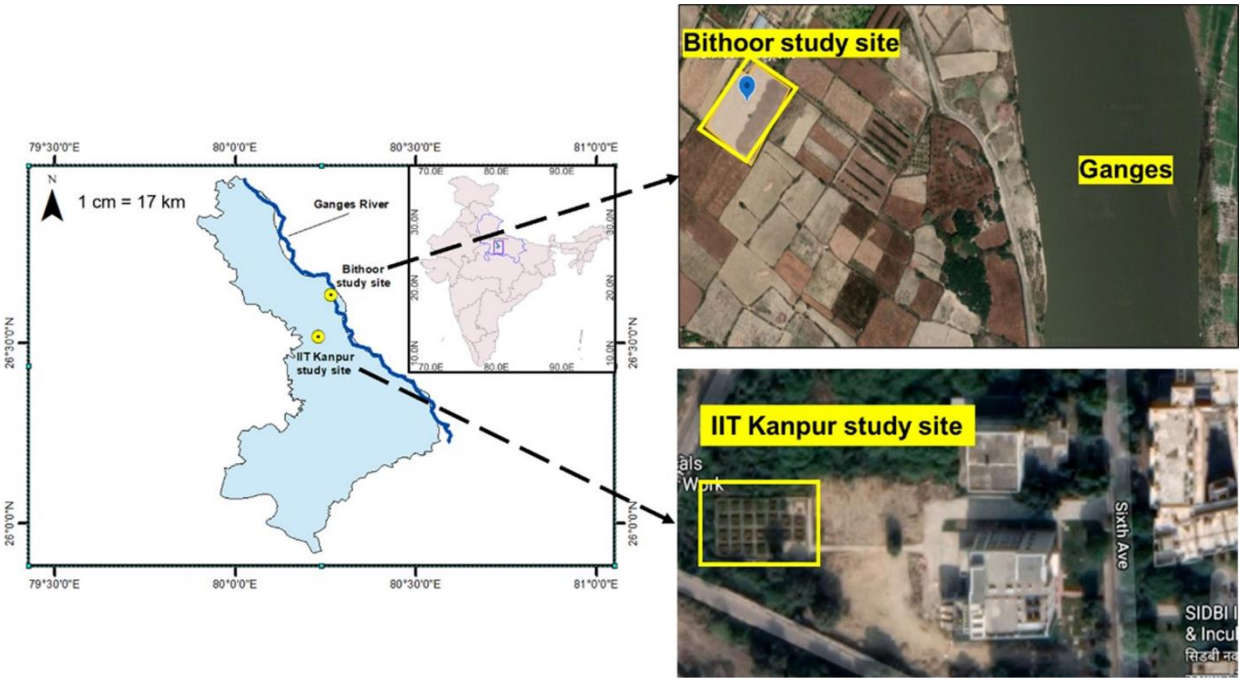

Figure 1: Geographical locations of the two experimental field sites: Bithoor and the IIT Kanpur study sites.

2. **Hydro-meteorological measurements:** Automatic weather stations were installed at the two sites to measure variables, including rainfall, air temperature, relative humidity, wind speed and direction, global solar radiation and soil heat flux (*Table A2*). All weather station data were collected at 15-minute intervals to capture diurnal variations effectively. At the Bithoor study site, air temperature and relative humidity were measured at three different heights to assess vertical variations in microclimatic conditions. Additionally, a CNR4 net

radiometer was installed to measure incoming and outgoing shortwave and longwave radiations. In addition to this, 5 temperature and relative humidity sensors were installed at each of the two sites along with 2 wind speed and wind direction sensors at different locations to assess spatial variation within the field. *Figure A1* provides a glimpse of instruments installed at one of the experimental sites.

3. **Agronomic practices for wheat and rice cultivation:** Wheat and rice were cultivated following standard agronomic practices prevalent in the study region. *Halna* variety for wheat and *DuPont Pioneer or Dhanyarekha* variety of rice were selected because of their popularity among the local farmers. Land preparation for both crops involved conventional tillage using hand tools or tractors. At the IIT Kanpur site, both chemical and natural/organic farming methods were adopted, while only organic farming was performed at the Bithoor site. In chemical farming, nutrient management included the application of Diammonium Phosphate (DAP) and Urea as fertilizers. In contrast, natural farming relied solely on *Jeevamrut*, a locally produced organic biofertilizer. Irrigation strategies varied significantly between the two crops. Wheat fields received 3 to 4 irrigations, each with an approximate depth of 60-70 mm, ensuring optimal moisture availability during critical growth stages. In contrast, rice fields were managed under a continuous flooding irrigation system, maintaining standing water throughout most of the growing season to support paddy growth and suppress weed competition. *Table A3* summarizes the agronomic practices followed in the study.

4. **Crop parameters:** *Table A4* details the timelines of wheat and rice cropping experiments conducted at the two sites. During the experiments, plant height was recorded weekly at five randomly selected locations per subplot at IIT Kanpur using a standard steel scale, with separate averages computed for organic and chemical treatments. At Bithoor, plant height measurements were taken at 15 randomly selected locations. Leaf Area Index (LAI) was measured using the LICOR LAI2200C canopy analyser, with measurements conducted in the evening to minimize solar interference. Each plot underwent two above-canopy and five below-canopy readings, and treatment-specific averages were computed. However, due to instrument malfunction, LAI data could not be collected in 2023.

5. **Measurement of evapotranspiration and evaporation using hydrometric methods:** Mini-lysimeters (150 mm diameter and 700 mm length), designed and fabricated at IIT Kanpur, were installed at both experimental sites to measure soil evaporation (E) and evapotranspiration (ET) (*Figure A2*). A total of fifteen mini-lysimeters were installed at each site, with nine dedicated to ET and six to E. These mini-lysimeters were equipped with an automatic weighing system that utilized load cells connected to in-house developed data loggers, ensuring high-frequency data collection at 15-second intervals. The data loggers employed ST microcontroller and ESP8266 for real-time data transmission (*Figure A3*). At IIT Kanpur, data were transmitted to an IIT Kanpur server via Wi-Fi, while at Bithoor, data was stored on memory cards. Additionally, 24 micro-lysimeters (100 mm diameter and 100 mm length) were installed at IIT Kanpur for manual measurement of soil evaporation. These measurements were conducted twice daily, at 10 AM and 5 PM. To maintain field conditions,

six micro-lysimeters were replaced daily, while the remaining eighteen were replaced every 4 to 5 days.

Raw load cell readings from mini-lysimeters often contain noise caused by environmental factors such as wind, temperature changes, and electronic noise. To address these issues, a systematic data processing approach was developed. The first step in the data processing pipeline was outlier detection and correction using the median absolute deviation method. This method is effective in identifying abnormal readings that deviate significantly from the expected pattern while remaining robust against extreme values. Once outliers were detected, they were replaced with the median value of the corresponding time window to prevent erroneous spikes or drops from distorting calculations. Following outlier correction, data averaging was performed to reduce random fluctuations and suppress high-frequency noise. Temporal averaging effectively cancels out short-term variations, ensuring a smoother dataset for further analysis. However, selecting an appropriate averaging window is crucial, as environmental conditions can change rapidly. An extensive analysis of mini-lysimeter data was conducted to identify an optimal averaging window. We followed the procedure given in Guide to the Expression of Uncertainty in Measurement (GUM) to quantify measurement uncertainty in E and ET.

6. **Isotope method for partitioning evapotranspiration:** The method involves collecting and analyzing atmospheric water, leaf water, xylem/stem water, soil water, rainfall and irrigation water for their isotopic signatures. The steps involved are briefly summarized below:

    a) **Water vapour collection using liquid nitrogen trap:** Atmospheric water vapour samples were collected using a setup designed to simultaneously capture vapour at five different heights (*Figure A4*). To achieve this, a liquid nitrogen trap-based air intake structure (AIS) was developed, ensuring efficient vapour collection while maintaining sample integrity. The AIS consisted of five temperature and relative humidity sensors, SHT85, which were chosen for their high accuracy and reliability. The SHT85 sensor provides a temperature accuracy of ±0.1°C and a relative humidity accuracy of ±1.5%. These sensors were mounted at different heights, which could be adjusted depending on the plant growth stage. The bottommost sensor was fixed at 0.15 m above ground, while the others were placed depending on the canopy height. This arrangement allowed for continuous monitoring of temperature and humidity at various heights, ensuring precise environmental data collection alongside isotopic sampling.

    b) **Soil and plant sample collection, transportation and storage:** Soil samples at multiple depths were collected from the field using a coring tool or by manually digging around the root zone. Care is taken to avoid contamination. A plant sample (typically stem or leaf) was obtained by carefully cutting them using sterilized scissors or a blade. The selection of plant parts was based on the objective of the study, as different parts may contain water with varying isotopic signatures.

Water from the collected soil and plant samples was extracted using a cryogenic vacuum distillation (CVD) setup, which included a heating water bath from where samples are heated and a distillation setup, which is emersed in liquid nitrogen, to condense the evaporated water. The efficiency of the sample extraction process by CVD was evaluated by estimating collection efficiency, extraction efficiency, and overall efficiency. The mean collection, extraction and overall efficiencies across all the samples for the developed CVD setup were estimated to be 94.95%, 99.64% and 94.44%, respectively. A comparison of these values with those reported in the literature showed that the developed CVD set-up performed effectively in extracting and recovering water from the soil and plant samples. *Figure A5* illustrates the steps involved in collecting soil and plant water samples.

c) **Isotope sample analysis:** The collected water samples were analyzed in a laser absorption spectroscopy based liquid water isotope analyzer (*Figure A6*). The analyzer was characterized to assess the memory effect, injected volume correction, and optimum analysis sequence. These factors were evaluated to ensure accurate and reliable isotopic measurements by minimizing biases caused by residual isotopic signatures, variations in injected volume, and instrumental drift. The precision of the isotope analyser was determined to be 0.39 ‰ for δ2H and 0.19 ‰ for δ18O.

d) **Isotopic composition of ET, E and T:** In this study, the Keeling plot method was selected to estimate the isotopic composition of evapotranspiration, δ_{ET}. This method assumes that the atmospheric water vapour in the boundary layer is the combination of background vapour already present and ET flux added locally to it. The isotopic composition of transpiration, δ_T, was obtained by measuring the isotopic composition of xylem water in the plant assuming the steady-state condition. The isotopic composition of soil evaporation, δ_E, is obtained by applying the Craig-Gordon model. Once the isotopic compositions δ_{ET}, δ_E and δ_T are known, then the transpiration fraction was calculated using a source linear mixing model as

$$F_T = \frac{\delta_{ET}-\delta_E}{\delta_T-\delta_E}.$$

NIH Roorkee

Table A5 lists the samples of different variables collected at NIH for isotope analysis during the project period. A brief description of the steps involved in collecting and analyzing the samples is provided in the subsequent paragraphs.

1. **Collection of atmospheric moisture samples:** Cooling the ambient air below its dew point and collecting the condensate is the traditional method of extracting moisture, the same was used in the present study by a locally developed instrument. The atmospheric moisture samples (n=668) were collected daily between 9:30 AM and 10:00 AM using cone-condensation techniques. Relative humidity is generally higher during this time as compared to day timings. The conical condensation apparatus comprises an aluminium cone, a metallic stand, and a lid. The cone is covered with a knob, and a cylindrical wire mesh cover protects the sample vials. Using the eight screws provided, the aluminium cone was

positioned so that the tip of the cone was directly above the bottle, and the moisture droplets condensing on the surface of the cone fell directly into the bottle (*Figure A7*). Depending on the prevalent relative humidity, it takes half to one hour for collecting 5 to 10 ml of liquid condensate. The location of the sampling was kept same for all study periods.

2. **Collection of plant transpiration samples:** Water transpires into the atmosphere by stomata and can be collected with transpiration bags (*Figure A8*). Water from plants is often taken from tissues before transpiration occurs to avoid any changes induced by increased isotope content owing to evaporation on the leaf surface. This method eliminates the need for destructive sampling, expensive laboratory equipment, training, and consumables. Furthermore, using bags is anticipated to generate a humid and warm environment, promoting isotopic equilibration while limiting evaporative enrichment. Selecting different plants for this experiment offers several advantages. Firstly, it ensures diversity in the study, as each tree species possesses unique characteristics and responses to environmental variables. This diversity allows for a broader understanding of how different trees interact with their surroundings. Secondly, experimenting with various species enables researchers to observe how trees adapt to different environmental conditions, providing insights into their resilience and suitability for various ecosystems and climate change. A total of 185 samples of transpiration were collected from four different plant species, namely, Ashoka tree (*Saraca asoca*), Indian laurel (*Terminalia elliptica*), Jamun tree (*Syzygium cumini*) and False Ashoka Tree (*Polyalthia longifolia*).

3. **Collection of soil evaporation samples:** Evaporation from bare soils constitutes the most substantial part of the hydrological balance in semi-arid regions. Several factors influence soil evaporation, including temperature, humidity, wind speed, solar radiation, soil moisture content, and soil type. The grass in these locations typically grows only during short rainy seasons; the rest of the time, it becomes dormant, senesced, or dies, exposing barren soil. An in-house experimental setup was created from a transparent acrylic sheet (5 mm thick) with dimensions of 75×75×60 cm to collect soil evaporation samples (*Figure A9*). It used an air compressor for suctioning and trapping evaporated vapours in the 50-ml glass tube kept in an icebox. The compressor is connected to a rotameter and nozzle valve to control the suction and trap processes. The suction process occurred at a rate ranging from 3 L/min to 5 L/min. The sample volume was found to be proportional to the suction rate. A Bluetooth data logger and a sensor to measure humidity and temperature variations were installed inside the experimental setup. A total of 221 evaporation samples were collected from December 2021 to December 2024.

4. **Collection of rainwater samples and development of Local Meteoric Water Line (LMWL):** It is crucial that the rainwater sample collected accurately reflects the overall natural precipitation during the specific sampling period. The choice of sampling equipment is often influenced by the accessibility and staffing available at the sampling site. Rainfall samples were collected for events. Each collected rainwater sample was stored in a 10 ml glass vial, with parafilm wrapped around the bottle to prevent evaporation. A standard non-recording rain gauge recommended by the IMD (Symon's rain gauge), depicted in *Figure A10*, was

employed to gather the 89 rainwater samples. These samples were also utilized in constructing the Local Meteoric Water Line (LMWL) for the region.

5. **Isotope analysis:** GV-Isoprime Dual Inlet Isotope Ratio Mass Spectrometer in the Nuclear Hydrology Laboratory of National Institute of Hydrology, Roorkee was used for measuring the stable isotopes (^{2}H or D and ^{18}O). The measured values are reported as delta (δ) values. The precision of measurement for $\delta\ ^{2}H$ is ± 1‰ and that for $\delta\ ^{18}O$ is ± 0.1‰. The primary standards used were VSMOW, GISP and SLAP, and secondary standards were Bisleri and Gangotri water. For ensuring the accuracy 3-points calibration was done for minimizing the errors and for doubtful results the samples are run in replicates. To ensure reliability of results, standards are run after every batch of the samples

III. Detailed Analysis of result

For brevity, only selected results are presented. As in the previous section, the tables and figures not included in the main report are provided in the appended and are denoted with prefix "A".

1. **Meteorological variables:** The seasonal trends of reference evapotranspiration (ETo), rainfall, and irrigation for wheat at IIT Kanpur and Bithoor during the 2023 and 2024 are shown in *Figure A11*. An increasing trend is seen in ETo with crop progression, reflecting higher atmospheric demand at later growth stages. Rainfall events were sporadic, with higher totals in 2024, particularly at Bithoor, which reduced irrigation requirements. IIT Kanpur received more irrigation than Bithoor, especially in 2023, due to delayed sowing, leading to increased evapotranspiration demand.

2. **Crop variables:** *Figure A12* illustrates the variation in wheat plant height at IIT Kanpur and Bithoor for 2023 and 2024 under different management practices. At IIT Kanpur, wheat grown under chemical treatment consistently exhibited greater plant height than under organic treatment, suggesting a growth advantage due to chemical fertilizers. In contrast, at Bithoor even with organic treatment, plants reached heights comparable to chemical treatment at IIT Kanpur. Inter-annual variations are evident, with wheat plants in 2024 showing slightly higher final plant heights than in 2023.

   Figure A13 presents the variation in Leaf Area Index (LAI) for wheat grown at IIT Kanpur and Bithoor. At IIT Kanpur, LAI exhibited a typical growth pattern - increasing during the early vegetative phase, peaking between 60–80 days after sowing (DAS), and then declining as the crop matured. The LAI under chemical treatment was consistently higher than under organic treatment, indicating that chemical fertilizers enhanced canopy development and leaf expansion more effectively.

   Figure A14 shows rice crop growth in 2023 and 2024 in terms of plant height and LAI at IIT Kapur. Chemically treated rice consistently exhibited higher plant height and LAI. The difference was more pronounced in 2023, indicating potential year-to-year variations in environmental conditions or fertilizer efficiency. Plant height showed a steady increase until

80–90 days after transplanting (DAT), while LAI peaked earlier before declining due to leaf senescence.

3. **Soil moisture:** *Figure A15* presents the temporal variation of surface soil moisture at a 10 cm depth, along with rainfall and irrigation events at IIT Kanpur and Bithoor for 2023 and 2024 wheat seasons. At IITK, soil moisture dynamics differed between chemical and organic fertilizer treatments, with chemical fertilizer plots generally exhibiting slightly lower moisture retention compared to organic treatments. Irrigation events significantly increased soil moisture, but the rate of depletion was higher in chemical fertilizer plots, possibly due to differences in water-holding capacity. At Bithoor, where only organic fertilizer was applied, soil moisture levels were generally higher and exhibited a gradual decline between rainfall and irrigation events, indicating improved moisture retention under organic treatment.

4. **Evaporation (E) and evapotranspiration (ET) estimation using hydrometric methods:** A stepwise data analysis framework (*Figure A16*) was developed to estimate ET. These included steps for outlier detection, smoothing, averaging, and aggregation. February 13, 2023, is chosen for illustration as high-speed wind was blowing on that day causing fluctuations in lysimeter data. The framework effectively removes noise, ensuring accurate ET estimation.

   Figure 2 presents lysimeter data for three days having distinct weather conditions, namely, foggy (January 1), rainy (January 22) and windy (February 13). Panel A shows normalized lysimeter weights. On January 1, the weight shows a steady but slow decline, indicating limited evaporation due to reduced solar radiation and low vapor pressure deficit. Panel B shows variations in ET, with the foggy day exhibiting the lowest ET (~0.1 mm/h) due to limited energy availability. The rainy day shows moderate ET (~0.2 mm/h) before rainfall but suppressed rates post-rainfall due to higher humidity. The windy day had the highest ET (~0.35 mm/h) as strong winds enhanced moisture transport. The uncertainty in estimating the rate of change of lysimeter weight reveals was highest for windy and rainy days (Panel C), emphasizing the impact of external disturbances. Panel D quantifies the influence of key lysimeter parameters—diameter (D), calibration factor (β_1), and slope of weight change (m) on ET uncertainty. Overall, the lysimeter effectively captures ET and environmental influences, with wind and rainfall introducing short-term variability in weight measurements, underscoring the need for careful calibration and uncertainty assessment in lysimetric ET estimation under dynamic conditions.

   Figure 3 illustrates the diurnal, intra-seasonal and inter-seasonal variability in E and ET for wheat at the Bithoor site. The figure highlights the responses to crop growth stages and prevailing weather conditions on ET partitioning. Over the entire crop season (November 19, 2023 – April 6, 2024), the total ET was 346.65 mm, with an average daily rate of 2.48 mm/day, while total soil evaporation (E) accounted for 191.39 mm (1.37 mm/day), and total transpiration (T) was 155.27 mm (1.11 mm/day). The transpiration fraction (T/ET) was 0.45. Panel A and B show diurnal variations in ET and E across different crop growth stages. In the early crop stage (late November to early January), a sharp peak in evaporation was observed between 10:00–12:00 hours, primarily due to the evaporation of dew and surface moisture

dissipation. During this period, E dominated ET, as the crop canopy was insufficient to drive substantial transpiration. The transition in the development stage (mid-January to early March) saw a decline in evaporation due to increased canopy coverage, reducing direct soil exposure to sunlight and wind. As a result, transpiration contribution in ET increases. The mid-season stage (March to early April) exhibited a clear dominance of transpiration, with a pronounced midday peak in ET. This phase coincided with rising temperatures, longer daylight hours, and a fully developed canopy, leading to maximum root water uptake. Soil evaporation was at its lowest during this stage, confirming that canopy shading effectively reduced direct soil moisture losses. The late-season stage, marked by leaf senescence, saw a gradual decline in ET as plant water uptake decreased.

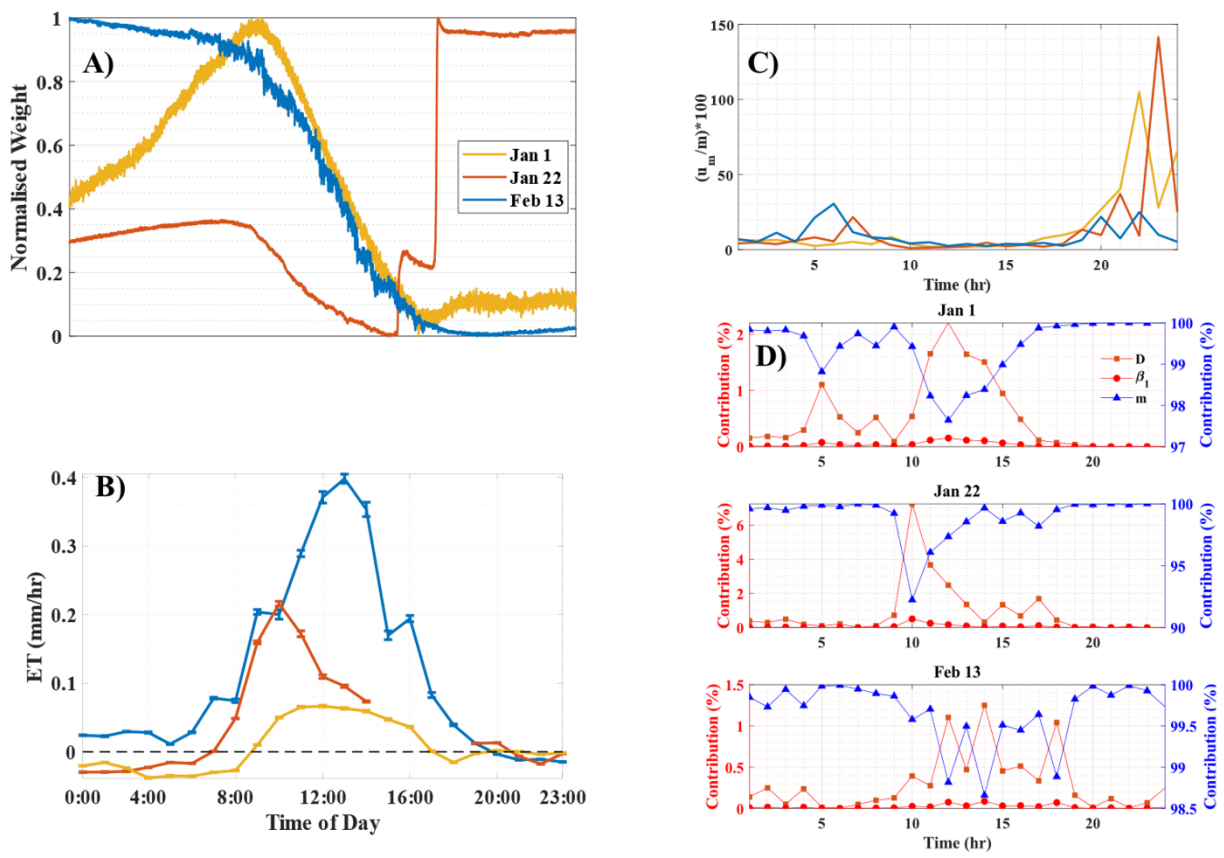

Figure 2: Lysimeter performance analysis on three contrasting days—January 1 (foggy day), January 22 (rainy day), and February 13 (windy day). (A) Normalized variations in lysimeter weights, (b) Estimated ET, (c) Percentage uncertainty in estimation of raw ET rate, i.e., slope of cthe lysimeter weight, and (d) Relative contributions of the uncertainties in estimation of diameter (D), calibration parameter (β_1), and slope of the lysimeter weight data (m) on the uncertainties of ET rate.

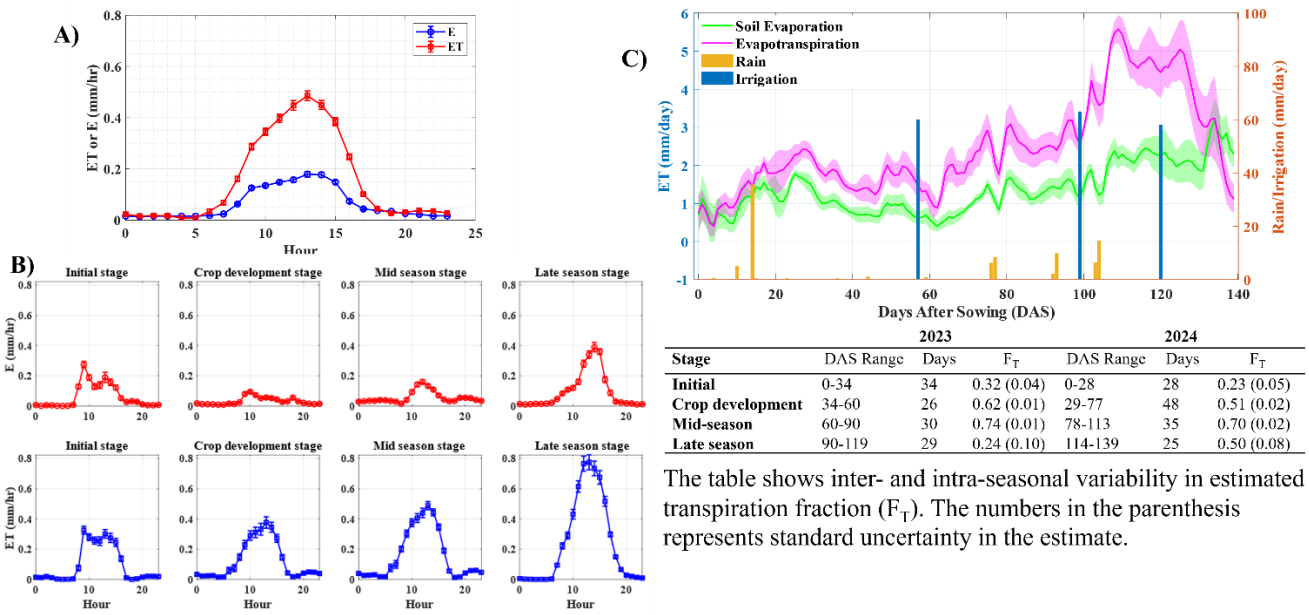

	2023			2024		
Stage	DAS Range	Days	F_T	DAS Range	Days	F_T
Initial	0-34	34	0.32 (0.04)	0-28	28	0.23 (0.05)
Crop development	34-60	26	0.62 (0.01)	29-77	48	0.51 (0.02)
Mid-season	60-90	30	0.74 (0.01)	78-113	35	0.70 (0.02)
Late season	90-119	29	0.24 (0.10)	114-139	25	0.50 (0.08)

The table shows inter- and intra-seasonal variability in estimated transpiration fraction (F_T). The numbers in the parenthesis represents standard uncertainty in the estimate.

Figure 3: Diurnal and seasonal variations of evapotranspiration (ET) and soil evaporation (E) in a wheat field. A) Hourly variation of ET and E, showing peak values around midday; B) Hourly ET and E across four distinct crop growth stages (Initial, Crop Development, Mid-Season, Late Season); C) Seasonal variation in E and ET.

Table A6 and the embedded table in *Figure 3* compares ET and its components for wheat crops in 2023 and 2024. Total ET in 2023 and 2024 was 337.93 mm and 346.65 mm, respectively, showing slight variability while maintaining similar partitioning trends. However, a notable difference was observed in soil evaporation, which was lower in 2023 than in 2024. This difference may be attributed to variations in meteorological conditions and time of sowing.

5. **Evaporation (E) and evapotranspiration (ET) estimation using isotopic methods:** The first step in isotopic analysis was development of a local meteoric water line (LMWL) for the Kanpur. The LMWL was estimated to be $\delta^2H = 7.96 \pm 0.09\ \delta^{18}O + 9.73 \pm 0.80$ ($R^2 = 0.98$ 6.11) and is shown as a dashed line in *Figure A17*. The figure also shows isotopic composition of water from rain, river, irrigation (ground water), soil, plant, dew and fog. The irrigation water from Bithoor and IIT Kanpur shows relatively higher $\delta^{18}O$ and δ^2H values compared to rainwater, indicating partial evaporation before application. The clustering of these data points suggests distinct sources at the two locations. River water, in contrast, has a more depleted isotopic composition, reflecting its primary dependence on precipitation with minimal evaporative losses. Soil water samples exhibit slight enrichment relative to rainwater, indicating evaporation before plant uptake. Leaf water exhibits the highest enrichment, as evaporation from the leaf surface preferentially removes lighter isotopes, leaving behind heavier isotopes. Stem water is relatively less enriched, suggesting direct uptake of soil water with minimal fractionation, though some influence of internal plant water transport mechanisms is evident.

Water vapor (WV) isotopic compositions at IIT Kanpur and Bithoor exhibit distinct site-specific variations, with a strong correlation between $\delta^{18}O$ and δ^2H at both locations (*Figures*

A18, A19 and A20). IIT Kanpur data shows a broader isotopic range, suggesting greater variability in atmospheric moisture sources, whereas the tighter clustering at Bithoor indicates localized isotopic control. The isotopic composition of WV varies with height, influenced by soil evaporation, plant transpiration, and atmospheric mixing. Regression slopes range from 4.19 to 5.10, with R^2 values increasing with height (0.50 at ground level to 0.77 in the upper canopy), indicating a transition from soil-dominated evaporation to transpiration-driven vapor. Near the ground, isotopic variability is higher due to kinetic fractionation, while the upper canopy reflects equilibrium fractionation associated with leaf transpiration.

Figure 4 illustrates the analysis of the Keeling plots across different time periods, highlighting key variations in the relationship between isotopic composition and water vapor concentration. During the morning period (9:10–10:45), the slope of the Keeling equation was highest (1.28), indicating a stronger dependency of δ on concentration, but the R^2 value (0.29) suggests a weak fit. The high intercept uncertainty (18.36) and percentage uncertainty (30.29%) reflect significant variability in the data, possibly due to fluctuating environmental conditions like changing humidity or temperature. Between 11:10 and 12:50, the R^2 value increased to 0.60, indicating a better fit, while the slope (0.78) was lower than in the morning. The intercept uncertainty (5.66) and percentage uncertainty (10.47%) were also lower, suggesting more stable conditions and improved confidence in the intercept estimate. This period likely had more consistent atmospheric mixing. In the early afternoon (1:30–3:00), the slope dropped significantly (0.18), indicating a weaker dependence of δ on water vapor concentration. The R^2 value (0.21) remained low, and the intercept uncertainty (2.98) was the lowest among all periods, leading to a percentage uncertainty of only 7.48%. This suggests that atmospheric conditions were relatively steady, with less variation in sources of evaporated moisture. The final period (3:30–4:30) showed a moderate slope (0.68) but the lowest R^2 value (0.12), indicating poor correlation. The uncertainty in intercept estimation increased sharply (15.35), resulting in the highest percentage uncertainty (33.84%). This period likely experienced rapid environmental changes. Overall, the midday period (11:10–12:50) provided the most reliable Keeling plot fit, while the late afternoon (3:30–4:30) showed the highest uncertainty. These variations highlight the influence of atmospheric stability and environmental conditions on the accuracy of isotopic measurements.

The isotopic composition of evaporation was calculated using the Craig-Gordon model, while the isotopic composition of transpiration was taken as isotopic composition of xylem water. *Figure 4C* summarizes the measured isotopic composition ET, E, and T. The results indicate an increasing trend in transpiration fraction from morning to afternoon, peaking at 0.87 (87%) between 13:30–15:00, suggesting that transpiration plays a more significant role in the afternoon compared to evaporation. The transpiration fraction was compared with hydrometric methods (*Figure 4D*), which revealed that the isotopic method generally yields higher values than the hydrometric method, with both showing an increasing trend over the day.

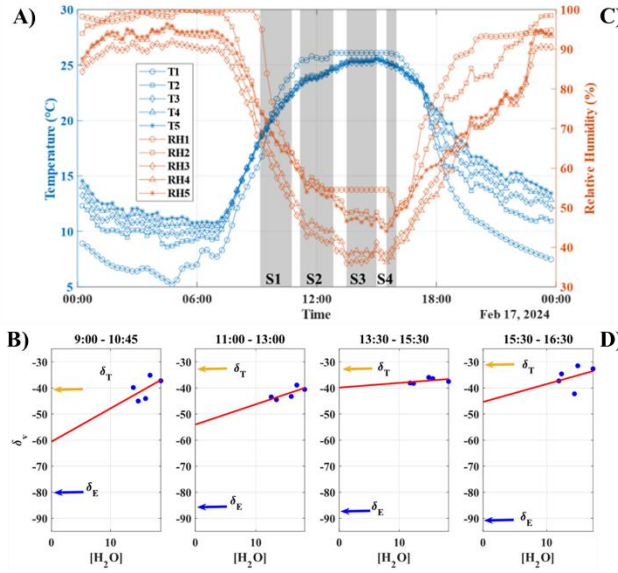

C)

Time	δ_E (‰)	δ_T(‰)	δ_{ET}(‰)	F_T
9:00-10:45	-80.78	-40.22	-60.61	0.50
11:00-13:00	-85.58	-32.98	-54.04	0.60
13:30-15:00	-87.64	-32.98	-39.86	0.87
15:30-16:30	-91.23	-29.31	-45.36	0.74

D)

Time	F_T (Hydrometric)	F_T(Isotope)
9:00-10:45	0.38	0.50
11:00-13:00	0.55	0.60
13:30-15:00	0.78	0.87
15:30-16:30	0.60	0.74

Figure 4: Diurnal variation of temperature, relative humidity, and isotopic partitioning of evapotranspiration on February 17, 2024 at Bithoor: (A) Temperature (T1–T5) and relative humidity (RH1–RH5) variations over the day, with shaded regions (S1–S4) indicating sampling time periods; (B) Isotopic δ values of vapor (δ_V) plotted against water vapor concentration ([H_2O]) for different time intervals, with δ_E and δ_T indicated on the plot; (C) Summary of the isotopic compositions (δ_T, δ_T, δ_{ET}) and transpiration fraction (F_T) at different time intervals; (D) Comparison of transpiration fraction (F_T) estimated by the hydrometric and isotopic methods.

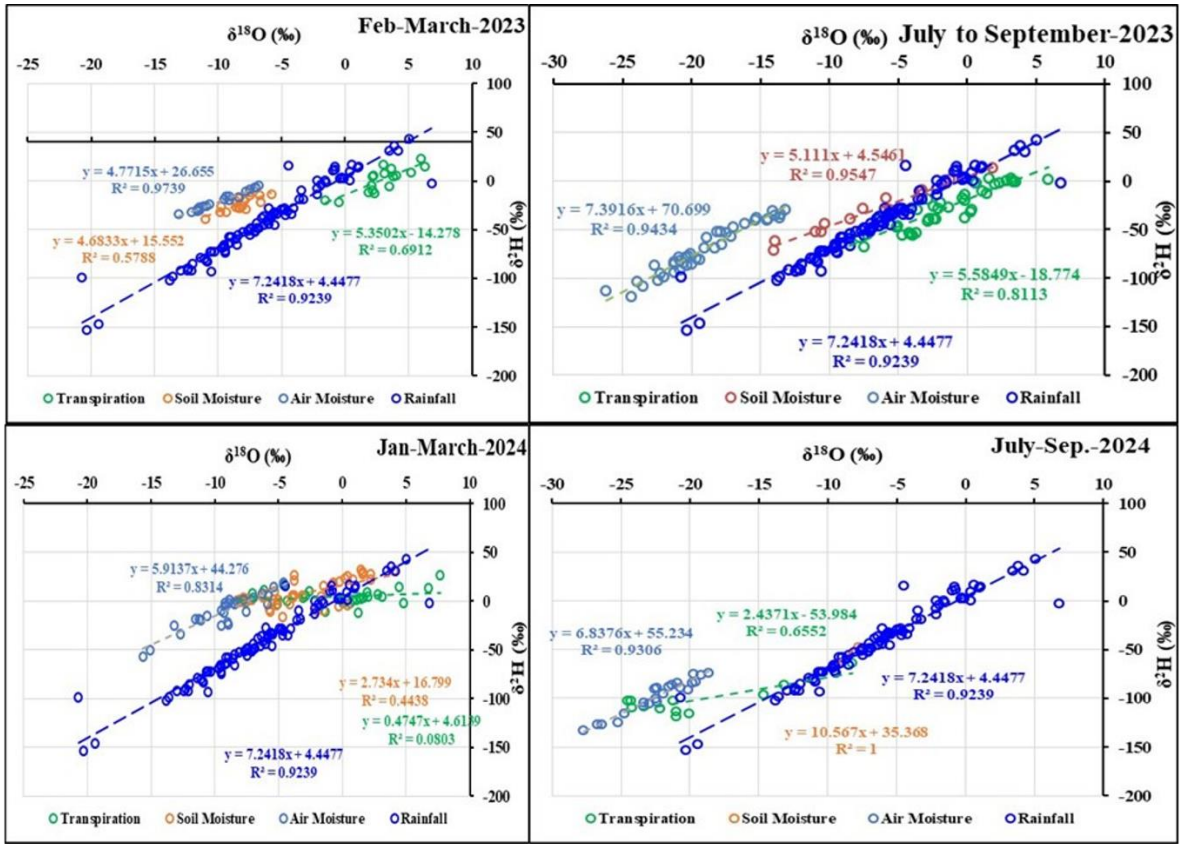

Figure 5: Scatter plot of isotopic composition ($\delta^{18}O$ vs. δ^2H) in the samples collected during 2023-2024 at NIH Roorkee for four time-periods. The parameters of the corresponding linear regression fit, and coefficient of determination (R^2) are also shown.

6. **Isotopic analysis of samples collected at NIH Roorkee**: The isotopic composition of samples collected during 2023-24 are presented and their implications ET and its partitioning are briefly discussed. A detailed report of the experiments conducted at NIH and the analysis of results are available at https://tinyurl.com/nihdetail

   (a) **Air moisture:** The isotopic composition of air moisture showed significant variability, with δ18O values ranging from -8.36 to -21.98 and an average of -20.17 (*Figure 5*; *Table A7*). The high correlation (R^2 = 0.9306) between δ18O and environmental parameters indicates that the isotopic composition is strongly influenced by factors such as temperature, relative humidity, and the source of moisture. The observed isotopic range suggests that air moisture in the study region is derived from a mix of oceanic and terrestrial sources, with significant fractionation occurring during condensation and re-evaporation. During the pre-monsoon season, the $\delta^{18}O$ ranges from -1.5‰ to 6.28‰, while the δD value spans from -113.23‰ to 4.44‰ (*Figure A21*). These values indicate a higher level of enrichment compared to the isotopic signature of air moisture observed in June and July. Additionally, in the monsoon season, the delta values exhibit a scattered distribution, ranging from -7.85‰ to 5.35 ‰, with a similar trend observed in the winter season.

   (b) **Soil Evaporation:** Soil moisture exhibited a narrow range of δ18O values, with an average of -8.60 (*Figure 5*; *Table A7*). The perfect correlation (R^2 = 1) suggests that soil moisture isotopes are highly predictable and primarily influenced by local precipitation and evaporation processes. The isotopic composition of soil moisture reflects strong isotopic equilibrium with rainfall. The narrow range of values indicates limited mixing with isotopically distinct sources, such as groundwater or surface runoff. This is a key observation, as it highlights the minimal contribution of external sources to soil moisture in the study area. The correlation between $\delta^{18}O$ and δD of the soil moisture evaporation for the summer season is excellent, despite limited data availability (*Figure A22*). The isotopic composition of the soil moisture evaporation for the monsoon season which has the variation of -13.98‰ to -5.41‰ also has good correlation. The $\delta^{18}O$ values vary between -14.04‰ to 1.85‰, indicating a mix of enriched and depleted data whereas during the pre-monsoon season, the data is concentrated within the range of -5‰ to -11.03‰.

   (c) **Transpiration:** Transpiration exhibited the largest range of δ18O values, with an average of -18.59 (*Figure 5*; *Table A7*). The moderate correlation (R^2 = 0.66) indicates that isotopic variations in transpiration are influenced by both environmental conditions and plant-specific factors. The wide range of values reflects significant isotopic fractionation during plant water uptake and evaporation at leaf surfaces. The correlation between $\delta^{18}O$ and δD for the summer months performs the best. In the monsoon seasons, the δ values are scattered, ranging from -7.85‰ to 3.34 ‰ (*Figure A23*).

(d) **Rain:** The isotope values showed a wide range, with an average of -9.51 (*Figure 5*; Table A7). The strong correlation (R^2 = 0.93) indicates that isotopic variations in rainfall are closely related to climatic factors such as temperature, altitude, and moisture source. The variability in δ18O values suggests contributions from different moisture sources, including oceanic and continental origins. Higher δ18O values correspond to local convective storms, while lower values are associated with large-scale monsoonal or orographic precipitation.

(e) **Temporal Variation of the isotopic signatures ($\delta^{18}O$) :** *Figure A24* shows that the isotopic signature of the transpiration is much more enriched than the isotopic signature of the air moisture. Whereas the isotopic signature of the soil moisture evaporation lies between that of the transpiration and the air moisture. The isotopic signature of rain is also plotted in the time series for June and July, 2023. We observed that whenever there was rainfall, it impacted the isotopic signature of other samples. Therefore, it can be said that rainfall plays a major role in the isotopic composition of air moisture, transpiration, and soil evaporation.

(f) **Effect of temperature and relative humidity in the isotopic signature:** The isotopic composition of water during evaporation and transpiration is primarily influenced by the composition of source water, atmospheric water vapor, relative humidity, and air temperature. While leaf conditions and plant parameters like stomatal conductance also play a role, they are less significant than atmospheric factors. Deuterium excess is particularly sensitive to relative humidity is therefore affected by evaporation process. Reduced humidity strengthens evaporation, leading to isotopically lighter water vapor in the atmosphere and heavier soil water. Consequently, plant-transpired water is typically isotopically enriched compared to soil-evaporated water, a characteristic used for ET partitioning.

IV. Conclusions

We have established two experimental sites at Kanpur for measuring ET flux and its components (Objective 1).

Experiments were conducted for wheat and rice during three cropping seasons. Instruments that were not commercially available or too expensive were developed in-house. Meteorological parameters at the two sites were measured by automatic weather stations. Crop parameters (e.g., plant height, root depth, leaf area index and above-ground biomass etc.) and water samples for isotope analysis were periodically collected. The water samples consisted of soil water, plant water, atmospheric water, irrigation water, groundwater, and rainwater. Experimental protocols were developed to – (a) optimally extract water from soil and plant samples without compromising their isotopic compositions and (b) determine the isotopic composition of collected water samples using laser-based isotope analyzer. The isotope data were used to develop a local meteoric waterline for

Kanpur and Roorkee. ET and its components were estimated for wheat and rice, as well as for four tree species. The data were analyzed to investigate diurnal, intra-seasonal and inter-seasonal variations in ET and its components. The transpiration fraction of ET was estimated using both hydrometric and isotopic methods, and the results were in agreement. The ET partitioning exhibited significant temporal variability and was found to be influenced by crop-growth stage, weather conditions, fertilizer treatment and irrigation. Experiments at NIH Roorkee revealed that soil evaporation during the post-monsoon period occurs concurrently with other hydrological processes, leading to a broader layer of isotopically enriched soil moisture. Consequently, plants transpire this enriched water, resulting in atmospheric water vapor with a heavier isotopic composition compared to the monsoon season (Objective 2)

The analytical precision of the isotope analyzer was determined to quantify uncertainty in the measurements of isotopic compositions. Further, a mathematical framework was developed to propagate uncertainties in isotopic and hydrometric measurements to estimated fluxes (Objective 3).

Overall, the project has provided insights into ET dynamics and partitioning in the rice-wheat system in the Upper Gangetic plains region. The study will also provide a theoretical and experimental basis for performing isotope-based ET partitioning studies in India.

V. Scope of future work

1. Design of lysimeter for seepage measurement: A lysimeter specifically designed to measure seepage losses, particularly during the rice-growing season, should be developed to improve water balance estimations.
2. Development of a Peltier element-based autosampler: A sampling system utilizing a Peltier element-based autosampler can be designed to collect atmospheric water vapor more efficiently for isotope analysis. Since it is very difficult to collect water vapor at remote location using liquid nitrogen based cold traps.
3. Exploration of in-situ methods for soil and plant water collection: Since cryogenic vacuum distillation is a destructive method, alternative in-situ techniques should be investigated for non-destructive isotope sampling of soil and plant water.
4. Direct analysis of water vapor using a water vapor isotope analyzer: The current approach relies on Keeling plots for isotope analysis, but these can be improved by directly analyzing water vapor using a field-deployable Water Vapor Isotope Analyzer.
5. Investigation of non-steady-state transpiration: The study assumed a steady-state transpiration, but in real-world conditions, this assumption may not always hold. Future research should focus on quantifying non-steady-state transpiration fraction dynamics for improved ET partitioning.
6. The data generated from both hydrometric and isotopic methods can be utilized for developing and testing hydrological models at plot and field scales, thereby improving future water conservation and agricultural planning strategies
7. Knowledge of isotopic compositions of different components of hydrological cycles and their temporal variations, as studied in this project, can be useful in understanding the complexities of hydrological processes in the Ganga basin. A long-term isotopic record can be helpful in deciphering the response of the hydrological cycle to climatic and anthropogenic changes.

Appendix

Tables

Table A1: Soil properties observed at the Bithoor and IITK study site*s* (Ksat – saturated hydraulic conductivity; OC - organic carbon; gd - dry density; G - specific gravity; and n – porosity)

Depth (cm)	**Location**	**Ksat (cm/day)**	**OC (%)**	**gd (g/cm³)**	**G**	**n**	**Sand (%)**	**Silt (%)**	**Clay (%)**	**d_{50} (mm)**	**Soil Type**
0-15	Bithoor	14.3	1.99	1.39	2.50	0.45	21.18	76.75	2.07	0.046	Silty-loam
	IITK	7.4	2.60	1.59	2.55	0.47	14.54	78.49	6.97	0.022	Silty-loam
15-45	Bithoor	12	1.72	1.44	2.48	0.44	21.2	76.06	2.74	0.043	Silty-loam
	IITK	8.93	1.53	1.61	2.56	0.44	13.87	78.74	7.39	0.020	Silty-loam
45-90	Bithoor	16	1.23	1.43	2.54	0.44	22.79	74.96	2.25	0.045	Silty-loam
	IITK	7.82	0.87	1.71	2.52	0.46	12.18	81.11	6.71	0.024	Silty-loam

Table A2: List of weather variables measured at the two study sites by automatic weather stations.

Variables	**Instruments**	**Location**	**Sampling rate**
Rainfall	Tipping bucket rain gauges	IITK and Bithoor site T and RH at two heights at IITK and 3 heights at Bithoor 2 Soil heat flux at each site Wind speed and wind vanes at 3 locations at each study site	15 min
Air T & RH	Thermometer and hygrometers		
Global solar radiation	Hach radiometer		
Soil heat flux	Soil heat flux plates		
Wind speed and direction	Anemometer and wind vanes		
Pan Evaporation	ISI class A Pan	IITK	
Soil temperature and moisture	SMEC 300 and SM 100 sensors	5 depths at multiple locations on both sites	

Table A3: Agronomic practices followed in the study for wheat and rice crop

Parameters	Wheat	Rice
Seed variety	Halna	DuPont Pioneer/Dhanyarekha
Seeding rate	150-200 kg/hectare	1 plant /hill
Tillage method	Hand tillage/ tractor	Hand tillage/ tractor
Fertilizer	DAP & Urea / Jeevamrut	DAP & Urea / Jeevamrut
Insecticide and Nematicide	Chlorpyrifos	Chlorpyrifos
Irrigation methodology	Generally 3-4 irrigation of about 60-70 mm depth	Flooded irrigation continuous flooding

Table A4: Details of timelines of wheat and rice cropping experiments at Bithoor and IIT Kanpur (IITK) sites (DAS – days after sowing; DAT – days after transplanting).

Description	2021	2022			2023			2024		
	Rice	Wheat		Rice	Wheat		Rice	Wheat		Rice
	IITK	Bithoor	IITK	IITK	Bithoor	IITK	IITK	Bithoor	IITK	IITK
Sowing/ Transplant	COVID	13/01	19/01	13/08	10/12	09/01	03/08	19/11	09/01	16/08
Harvesting		13/04	23/04	05/12	08/04	20/04	17/11	06/04	23/04	19/11
DAS / DAT (days)		90	94	114	119	101	106	139	105	108

Table A5: Details of samples collected at NIH Roorkee for isotope analysis.

Sample number	Sample	Number	Method	Period
1	**Atmospheric air moisture**	668	Condensation	December 2021 to December 2024
2	**Transpiration**	185	Transpiration bag	February 2022 to December 2024
3	**Evaporation**	221	Soil evaporation sample collector	November 2021 to December 2024
4	**Rain**	89	Ordinary rain gauge	July 2022 to September 2024
5	**Source water**	34	Sampling	
Total		1197		

Table A6: Seasonal total and average daily evapotranspiration (ET), transpiration (T), and soil evaporation (E) for wheat in 2023 and 2024 for Bithoor.

	2023		**2024**	
Components	**Seasonal total (mm)**	**Avg (mm/day)**	**Seasonal total (mm)**	**Avg (mm/day)**
ET	337.93 (6.86)	2.82 (0.06)	346.65	2.48 (0.04)
T	206.16 (8.11)	1.72 (0.07)	155.27	1.11 (0.05)
E	131.77 (4.34)	1.09 (0.04)	191.39	1.37 (0.03)

Table A7: Isotopic characteristics of water samples collected at NIH Roorkee.

Source	**$\delta^{18}O$ (Range)**	**$\delta^{18}O$ (Average)**	**Regression Line**
Air moisture	-8.36 to -21.98	-20.17	$R^2 = 0.9306$ n =110
Soil moisture	-7.80 to -9.41	-8.60	$R^2 = 1$ n = 4
Rainfall	-2.19 to -20.72	-9.51	$R^2 = 0.9239$ n = 36
Transpiration	-8.24 to -24.56	-18.59	$R^2 = 0.6552$ n = 18

Figures

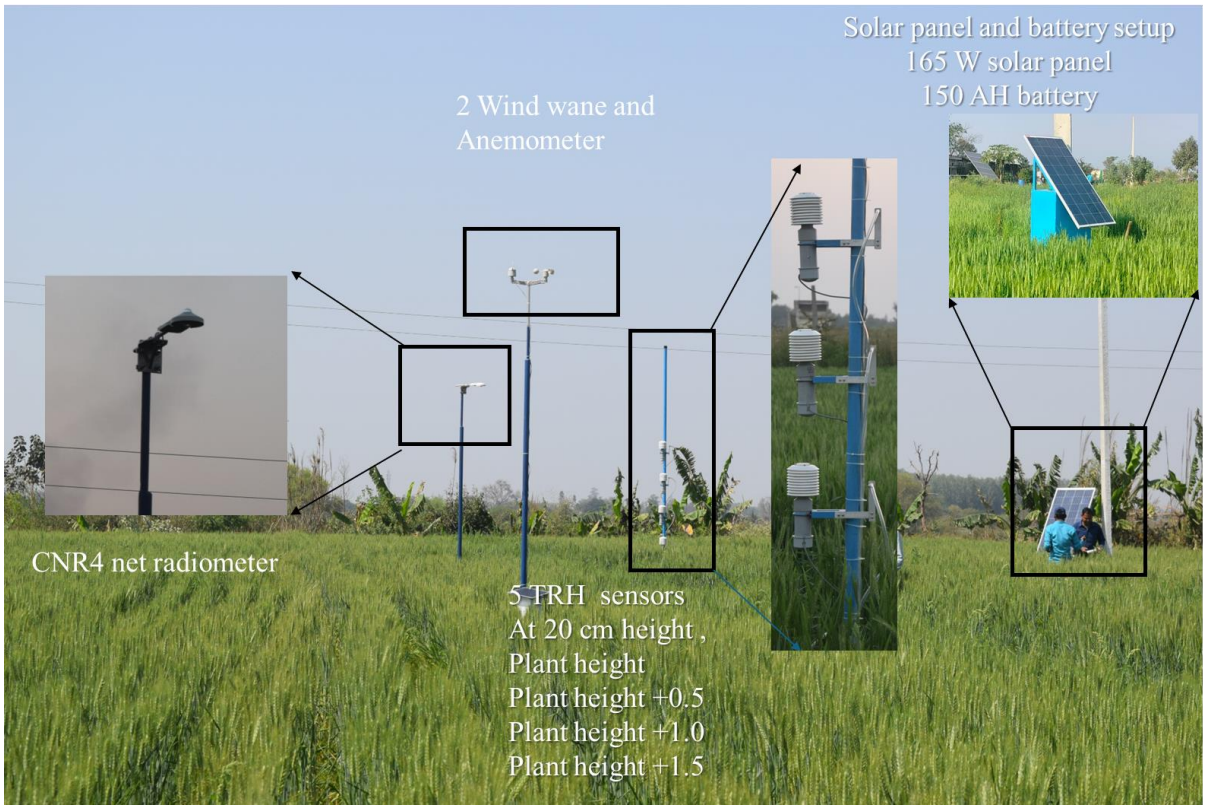

Figure A1: Instruments installed at the Bithoor study site.

Figure A2: Mini-lysimeter installed in a wheat field at Bithoor. The lysimeter setup is used for continuous monitoring of evapotranspiration (ET) by measuring real-time weight changes in the soil-plant system. The setup includes a high-precision load cell, data logging system, and a protective enclosure.

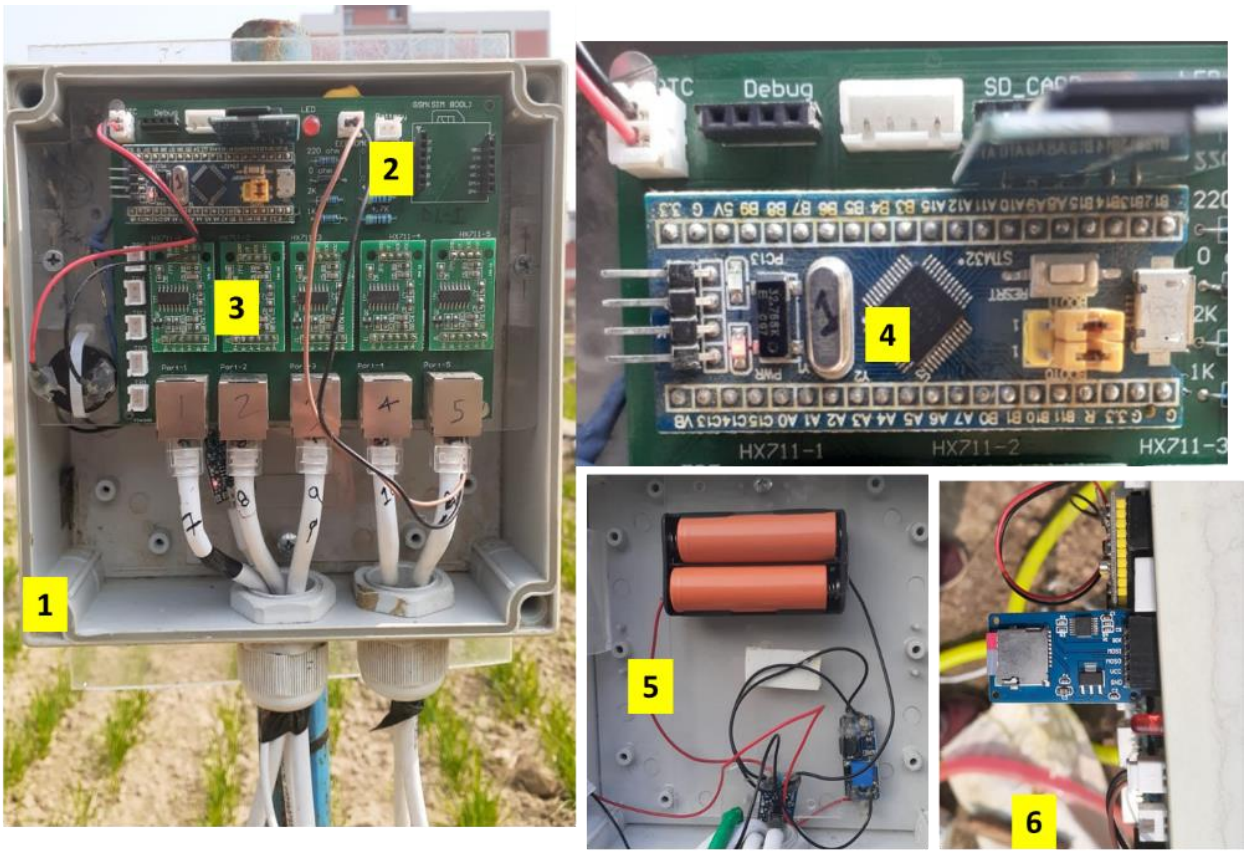

Figure A3: Developed data logger and its installation in an IP66 enclosure (1). The data logger includes a custom PCB (2); with all necessary components installed, such as HX711 load cell amplifiers (3); an ST microcontroller (4); 18650 batteries with a charging circuit (5); and an SD card module (6).

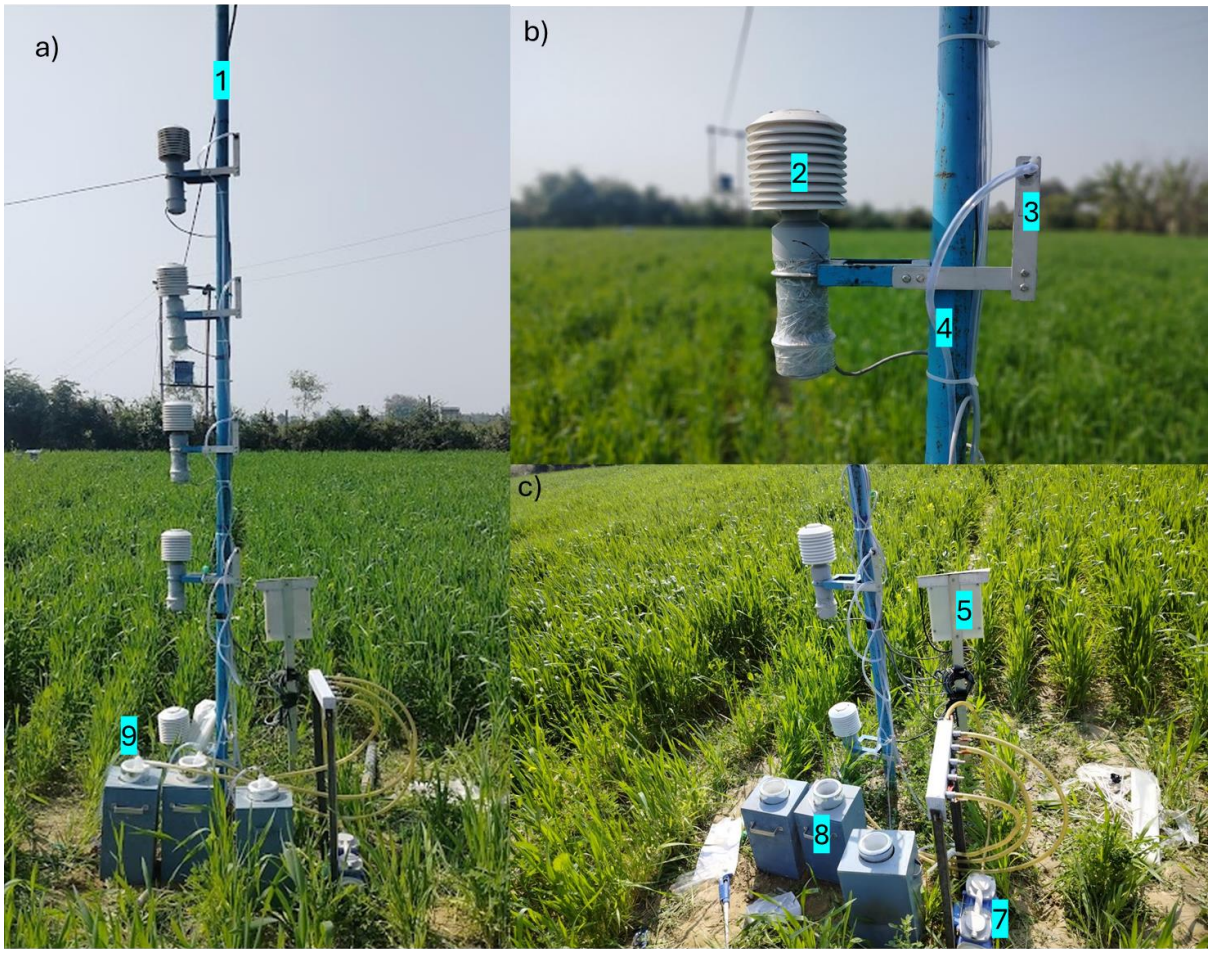

Figure A4: Setup for collection of water vapour. 1) Air Intake structure; 2) Temperature and relative humidity (T and RH) sensor with thermal shield; 3) Sampling port; 4) Teflon tube for sampling air moisture; 5) Data logger for T and RH sensors; 6) Manifold; 7) Vacuum pump; 8) Wooden box for holding Dewar flask; and 9) Cold trap.

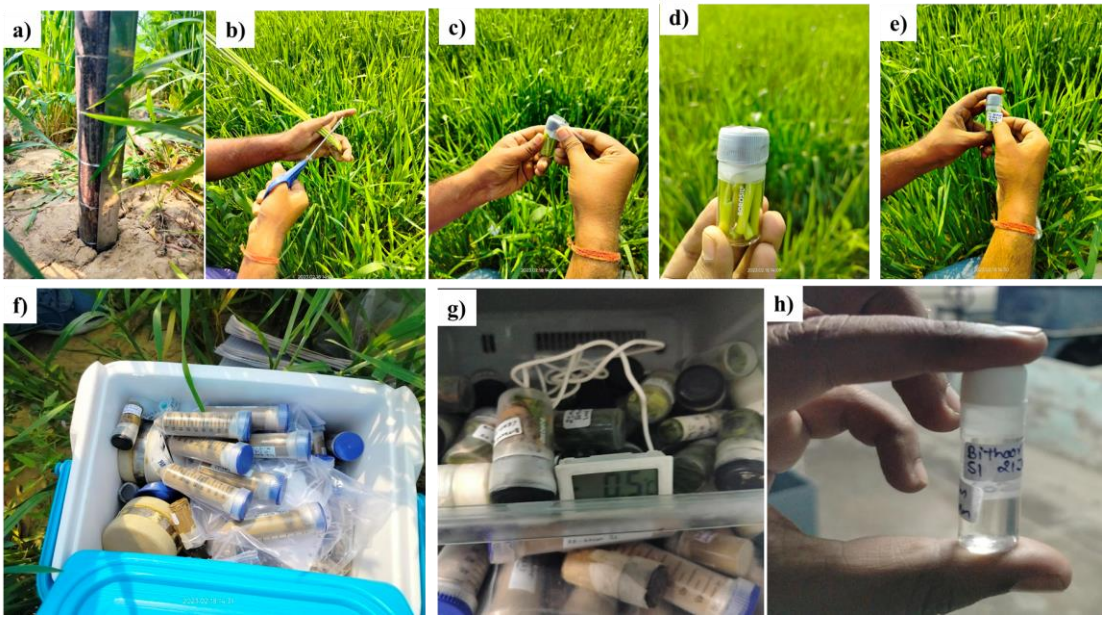

Figure A5: Steps involved in collecting and processing soil and plant samples for isotopic analysis: a)Soil sample collection; b) Cutting of plant sample; c) wrapping of parafilm; d) final sample collection; e) labelling of sample; f) Storing sample for transportation; g) storing in refrigeration; h) final sample extracted after cryogenic vacuum distillation.

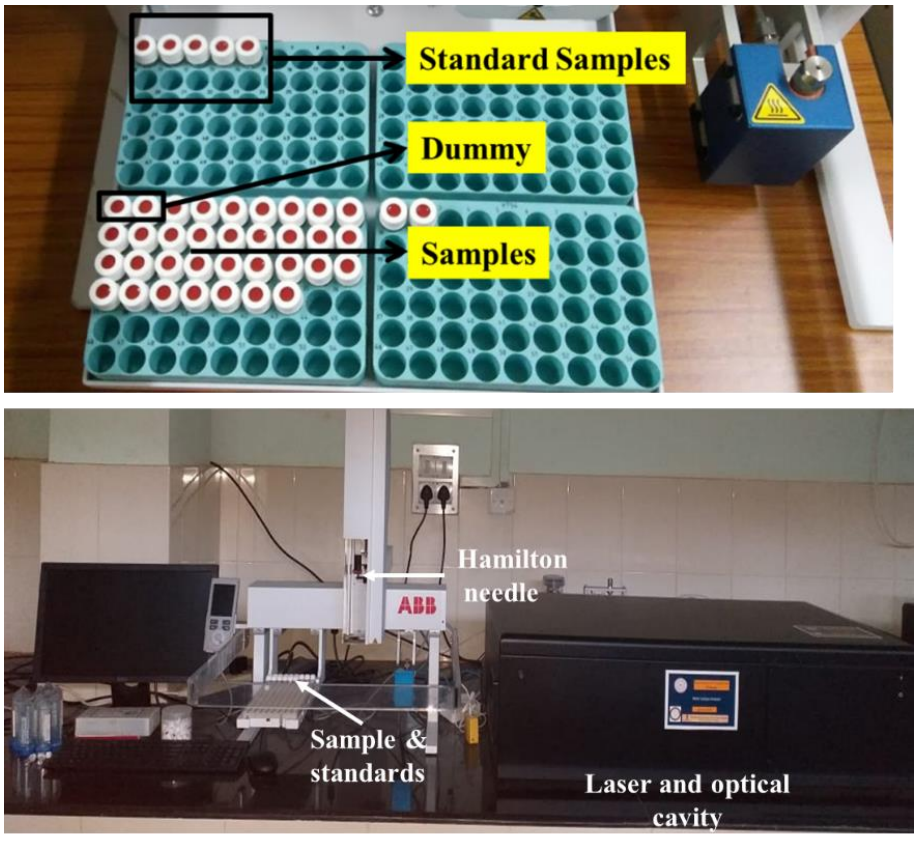

Figure A6: Laser absorption spectrometry based liquid water isotope analyzer.

Figure A7: Apparatus for collecting atmospheric moisture samples.

Figure A8: Process of collecting transpiration samples.

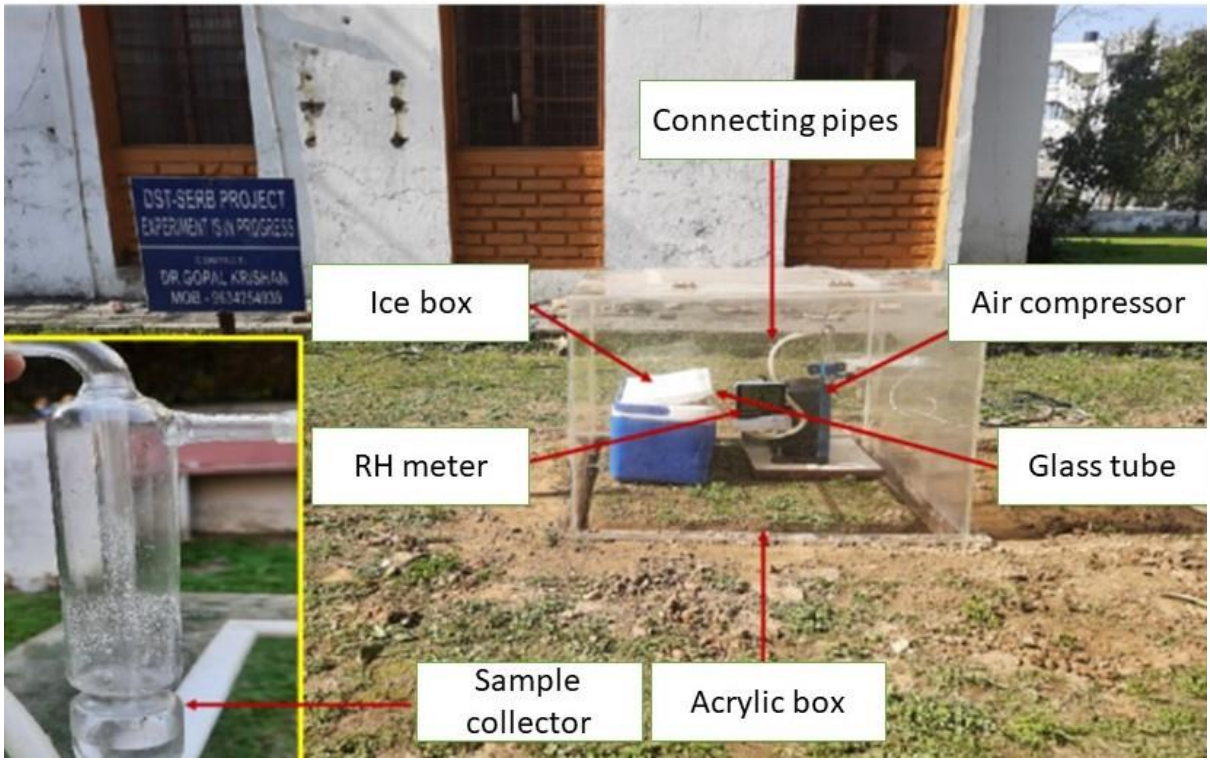

Figure A9: Set-up developed for collecting soil evaporation samples.

Figure A10: Rain gauge setup for collecting rainwater for isotope analysis.

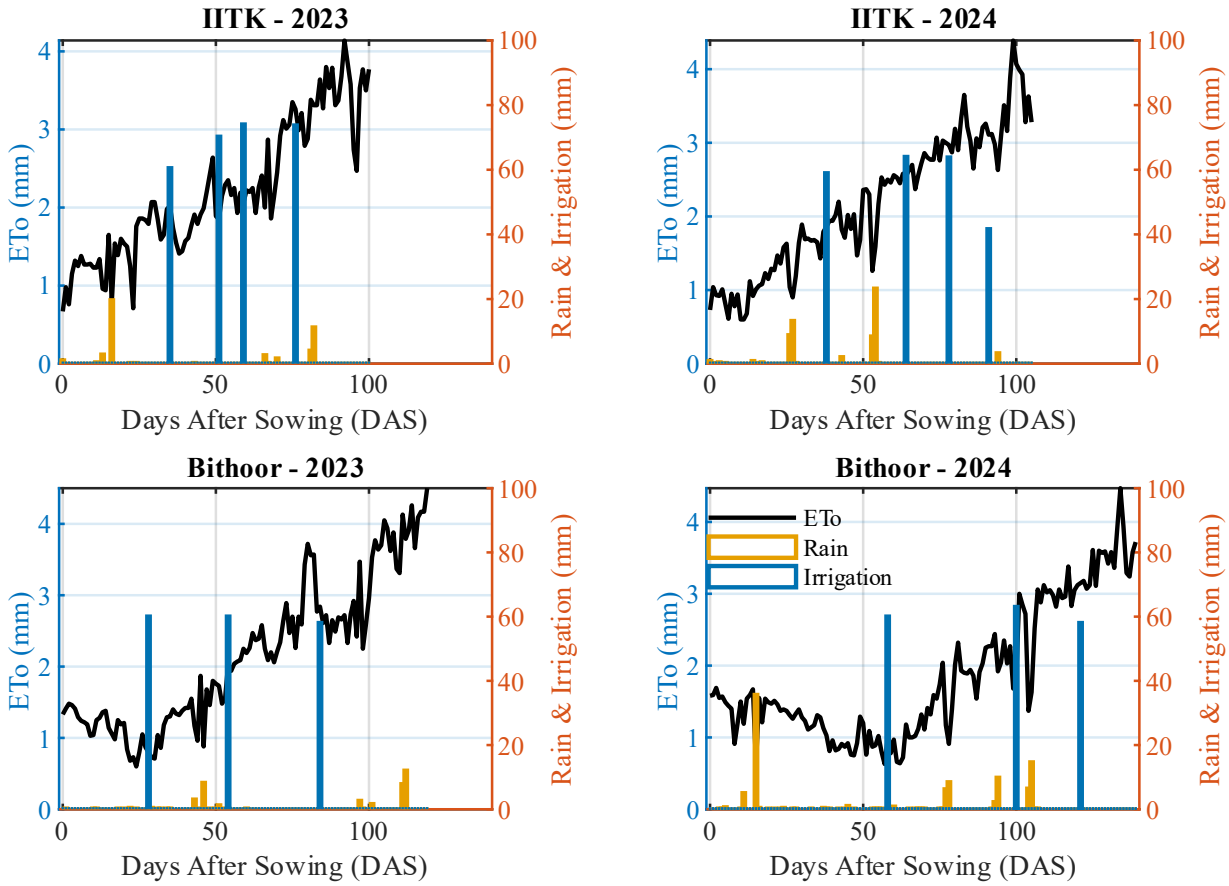

Figure A11: Seasonal variation of reference evapotranspiration (ETo), rainfall, and irrigation for wheat at IIT Kanpur (IITK) and Bithoor during the 2023 and 2024 growing seasons. The black line represents ETo (mm), blue bars indicate irrigation events, and orange bars represent rainfall.

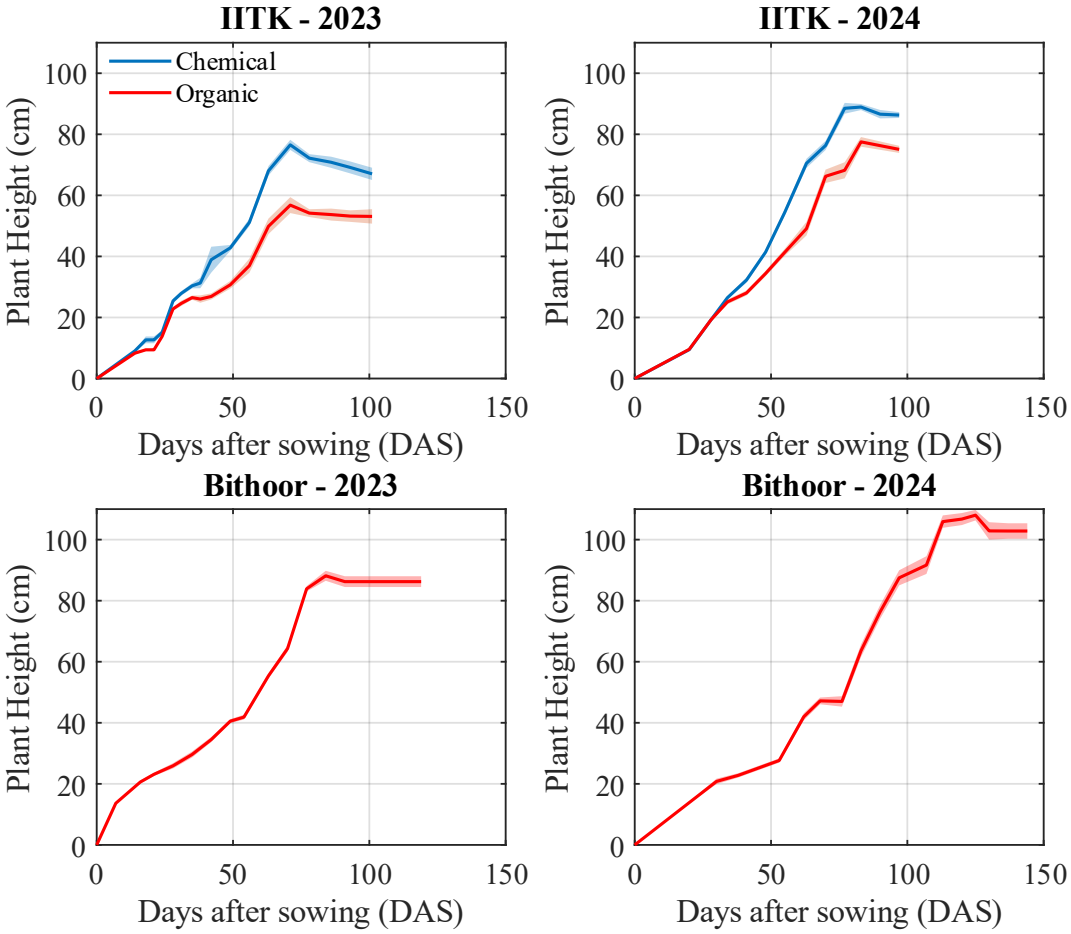

Figure A12: Growth trends of wheat plant height (cm) at IIT Kanpur (IITK) and Bithoor during the 2023 and 2024 growing seasons. The blue line represents chemical treatment, and the red line represents organic treatment.

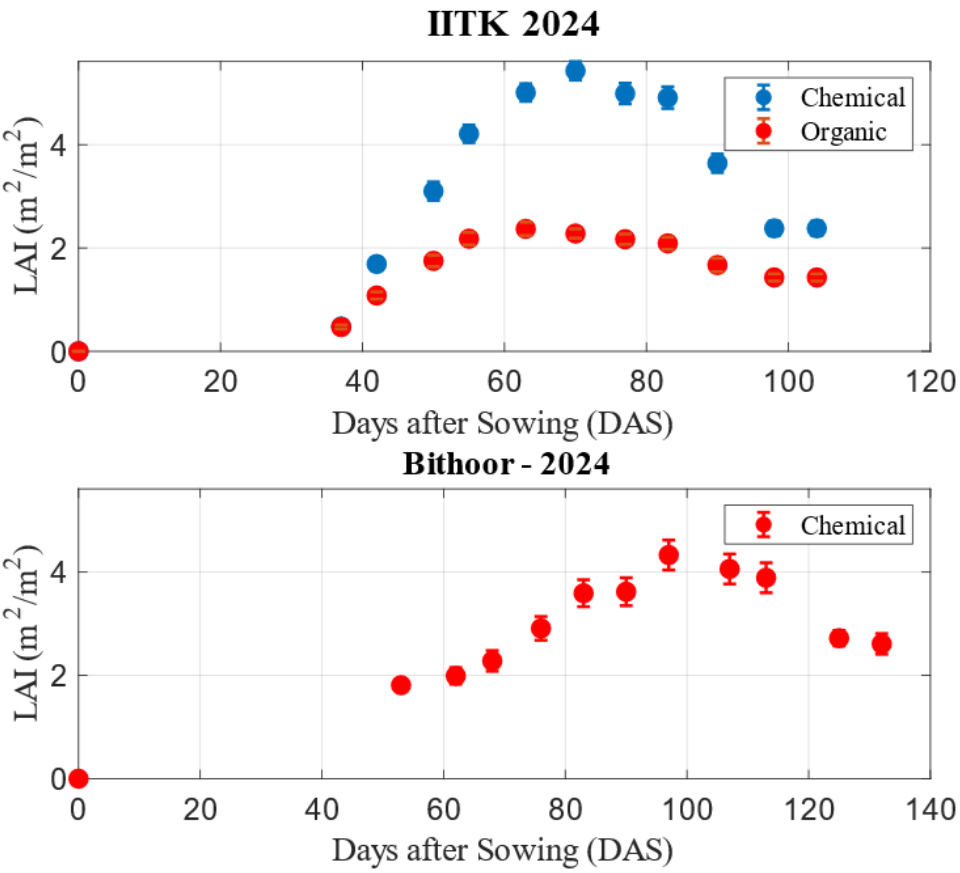

Figure A13: Variation in Leaf Area Index (LAI) with days after sowing (DAS) for wheat under different fertilization treatments at IIT Kanpur (IITK) in 2024 and at Bithoor in 2024

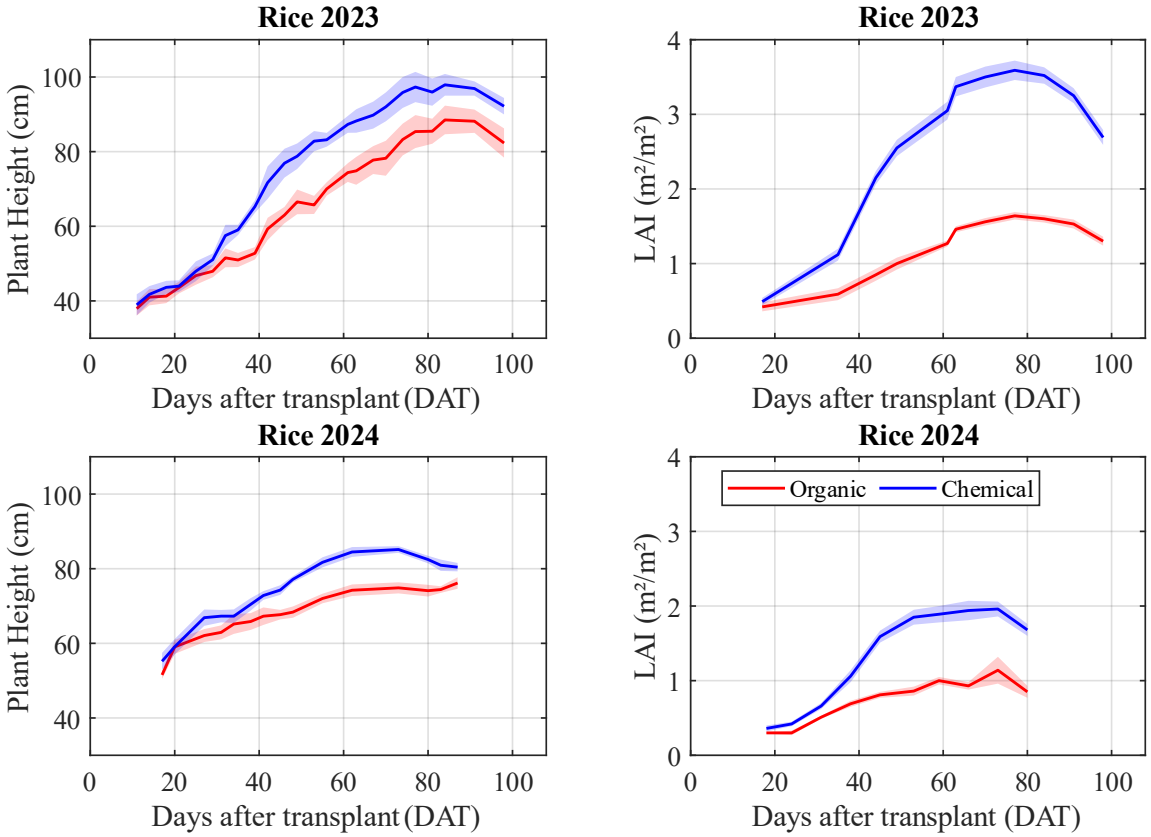

Figure A14: Variation in rice plant height and leaf area index (LAI) with days after transplanting (DAT) the paddy plant in agricultural plots with organic and chemical treatment.

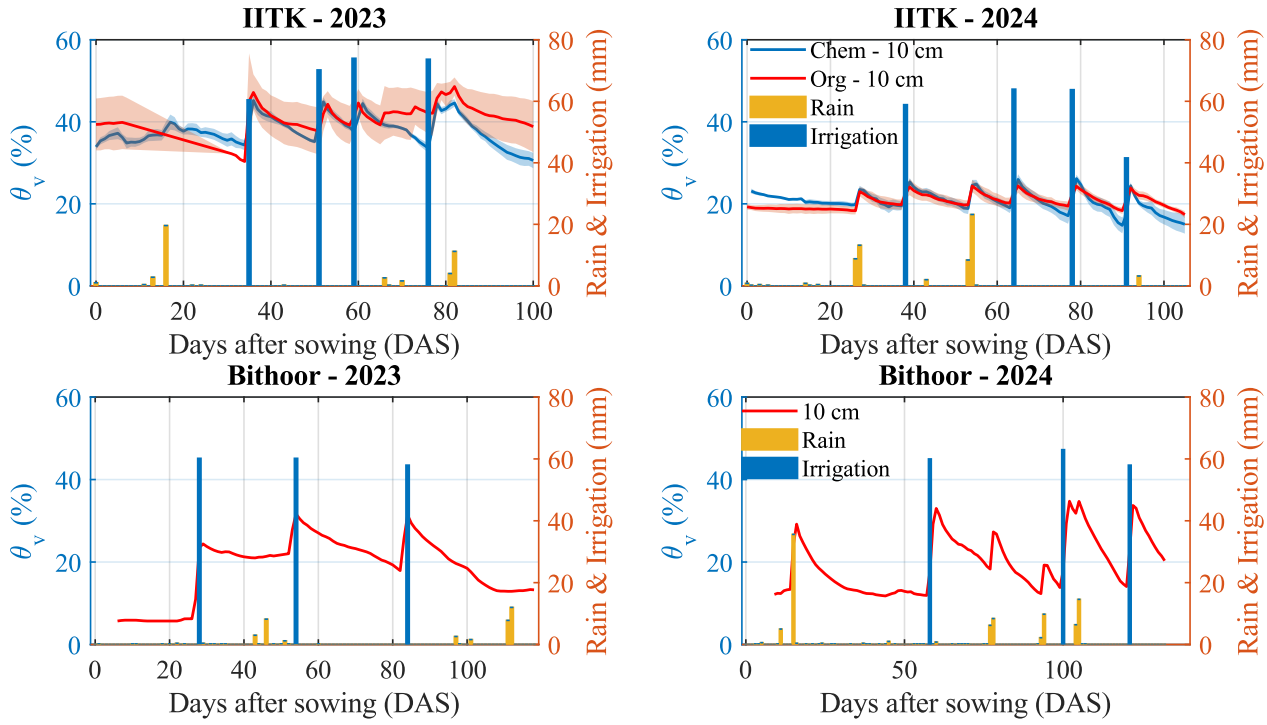

Figure A15: Temporal variation of surface soil moisture (θv) at 10 cm depth with rainfall and irrigation events at IIT Kanpur (IITK) and Bithoor during 2023 and 2024 wheat seasons.

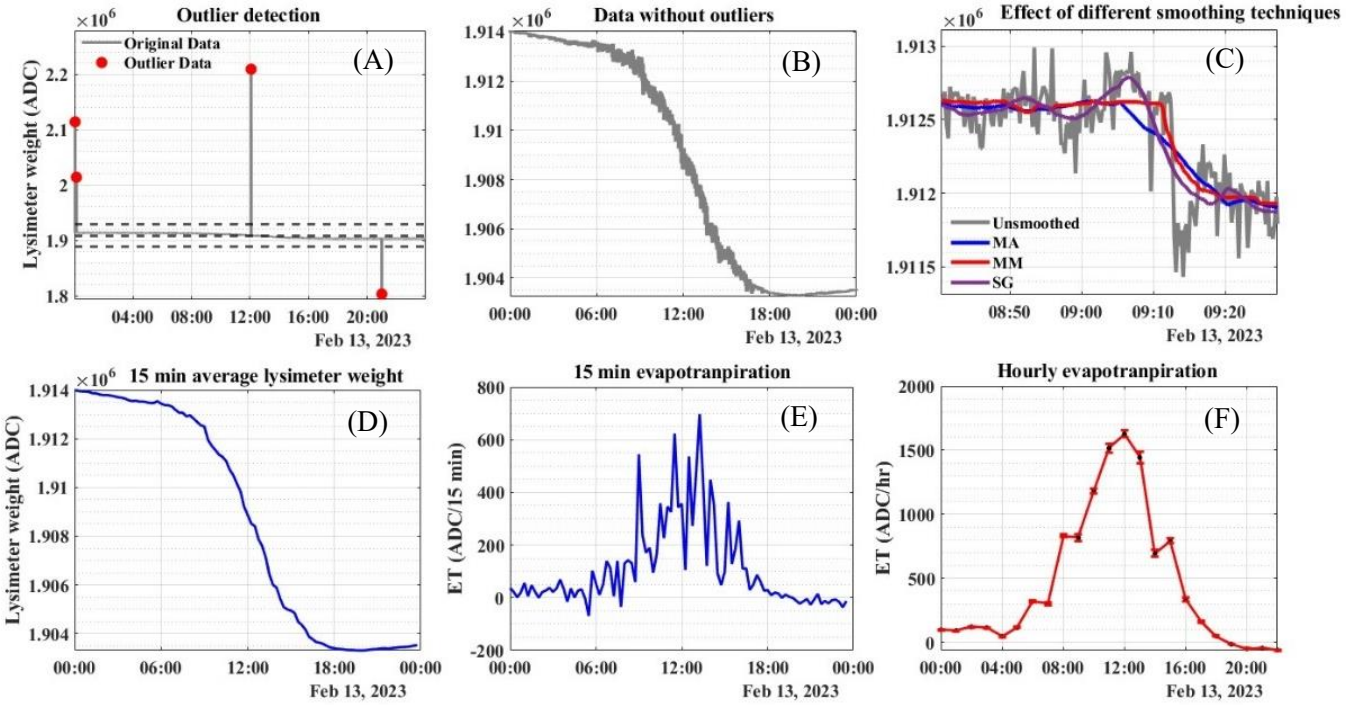

Figure A16: Processing of lysimeter data and estimation of evapotranspiration (ET) on February 13, 2023. Top row: (A) Outlier detection in lysimeter weight data, (B) Data after outlier removal, and (C) Effect of different smoothing techniques (MA: Moving Average, MM: Moving Median, SG: Savitzky-Golay fliter). Bottom row: (D) 15-minute average lysimeter weight, (E) ET estimated at 15-minute intervals, and (F) Hourly ET estimation.

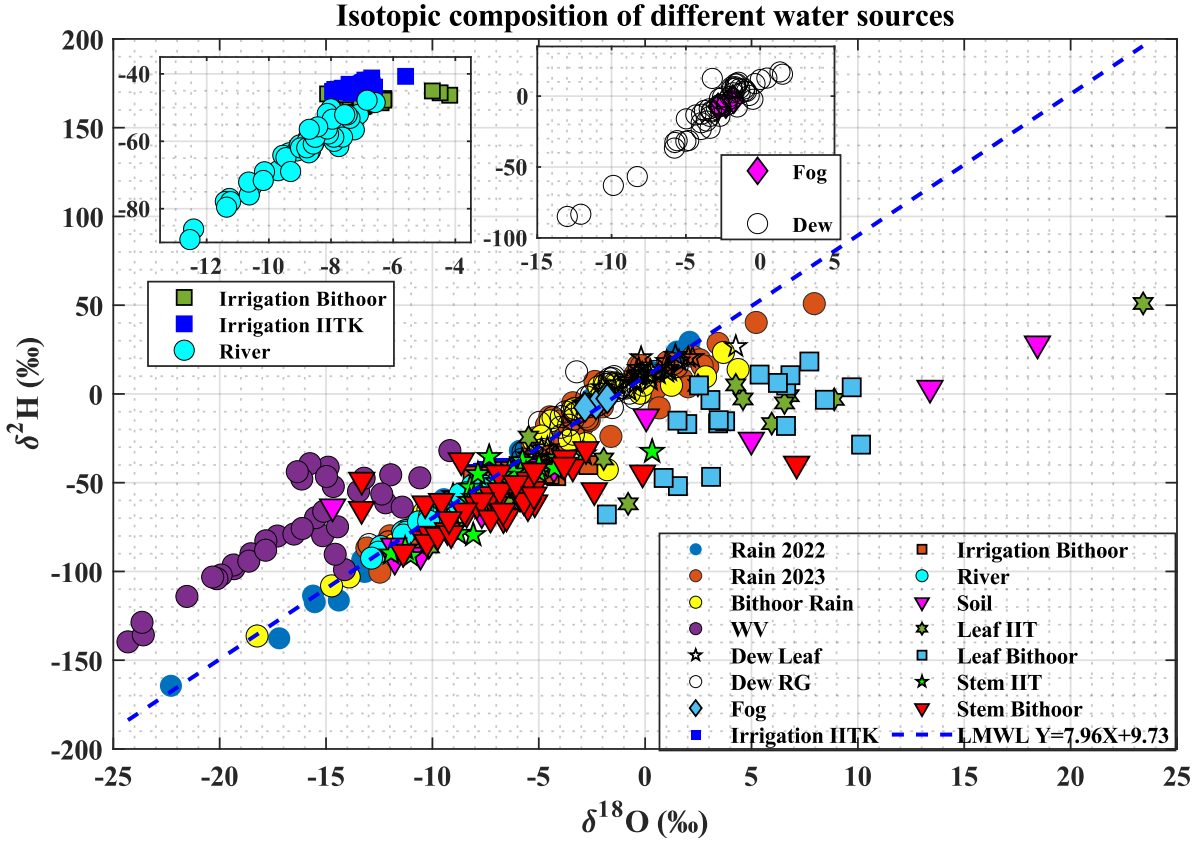

Figure A17: The local meteoric water line (LMWL) at Kanpur along with isotopic composition of different water sources at IIT Kanpur (IIT) and Bithoor sites (WV – water vapour; RG – rain gauge).

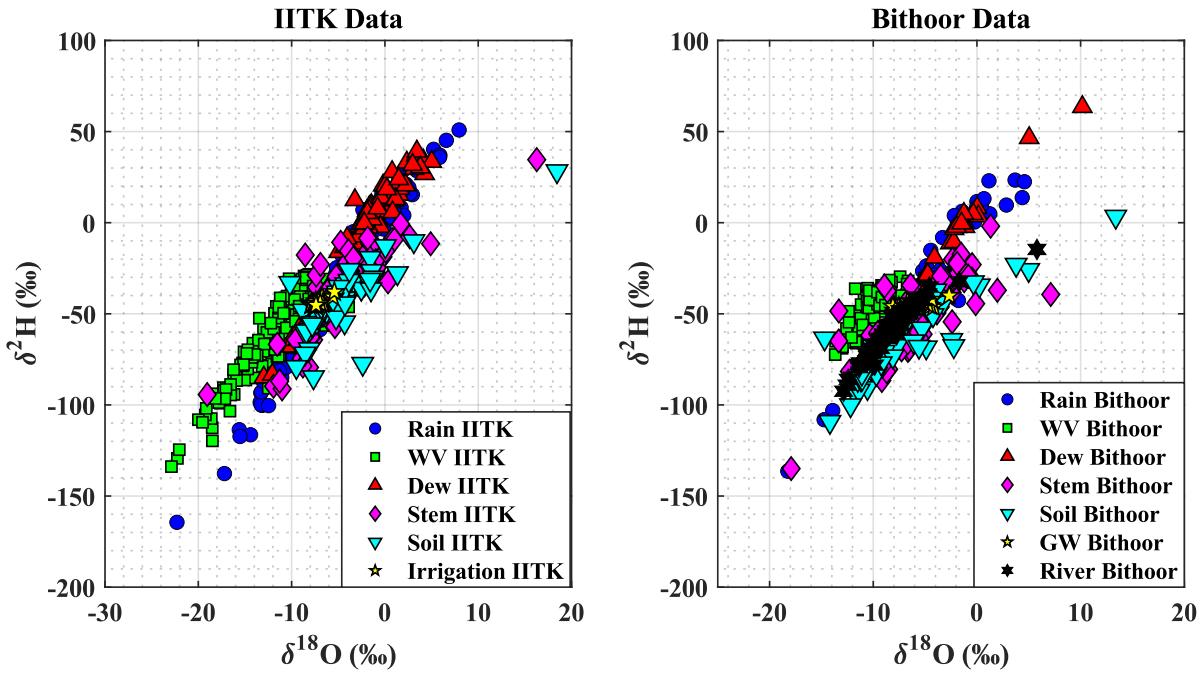

Figure A18: Comparison of isotopic composition ($\delta^{18}O$ vs. $\delta^{2}H$) of different water sources at IIT Kanpur (left) and Bithoor (right). The data includes rainwater, water vapor (WV), dew, plant stem water, soil moisture, groundwater (GW), river water, and irrigation water.

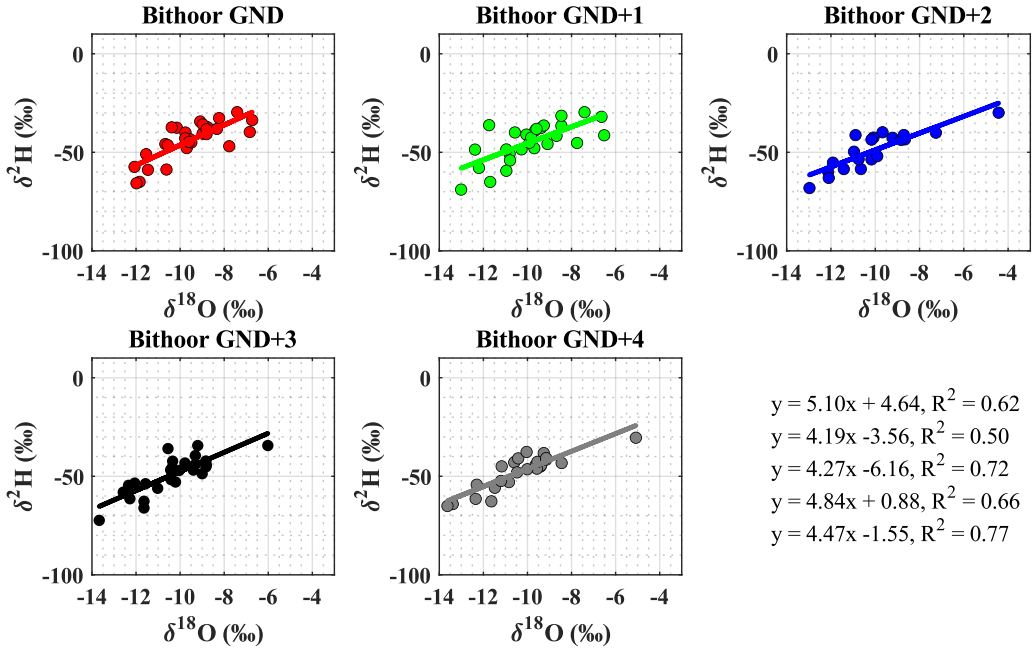

Figure A19: Scatter plot of isotopic composition ($\delta^{18}O$ vs. $\delta^{2}H$) of water vapour at Bithoor at different heights from the ground (GND) and the corresponding linear regression fit. GND+*h* denotes water vapour samples collected at *h* m above the ground surface.

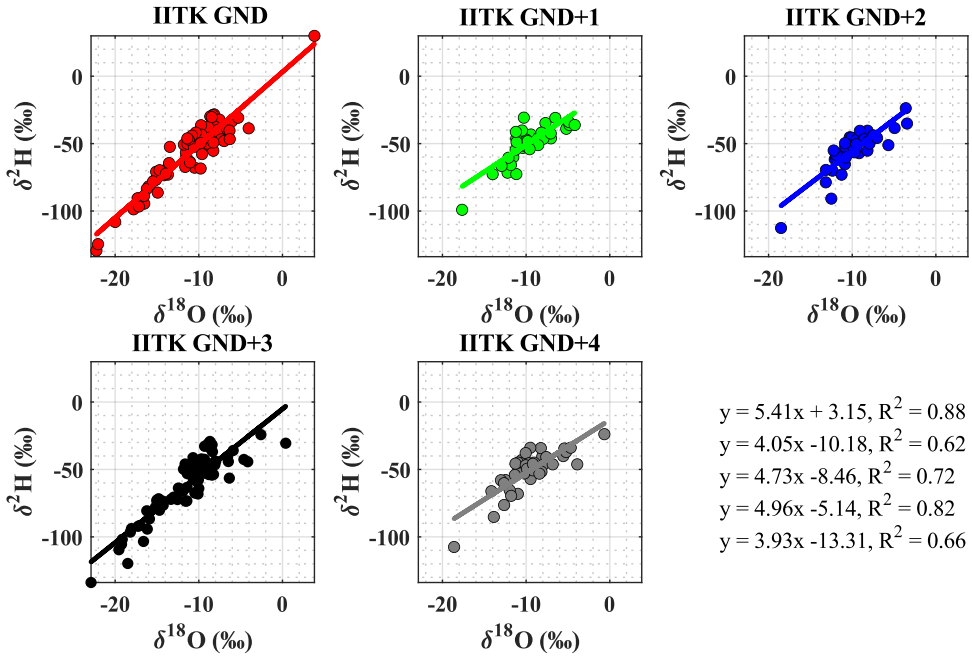

Figure A20: Scatter plot of isotopic composition ($\delta^{18}O$ vs. $\delta^{2}H$) of water vapour at IT Kanpur at different heights from the ground (GND) and the corresponding linear regression fit. GND+*h* denotes water vapour samples collected at *h* m above the ground surface.

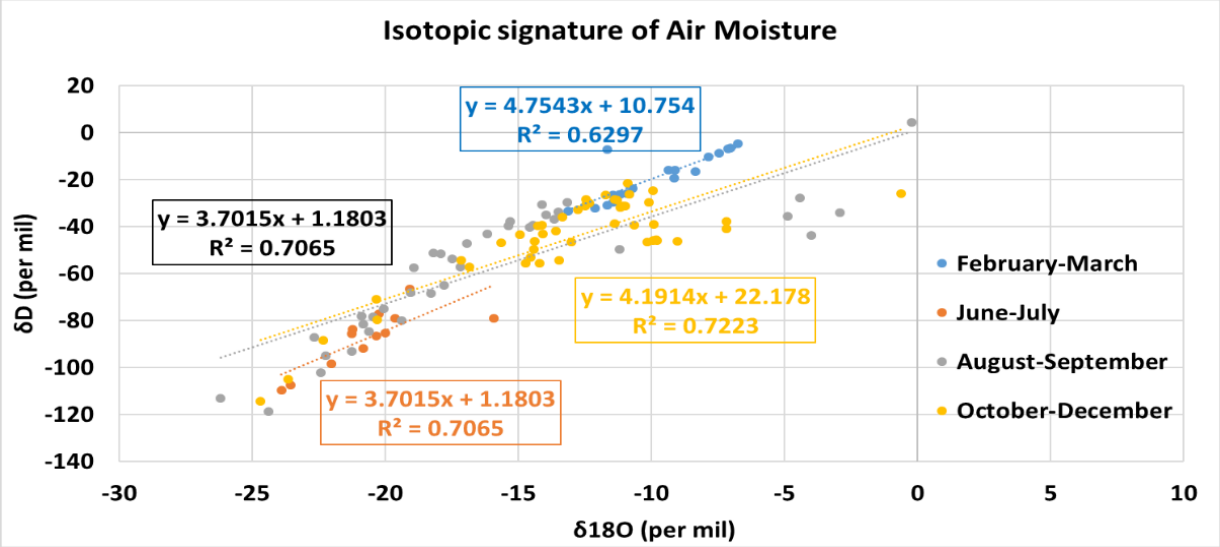

Figure A21: Seasonal variations of isotopic signature (δ ^{18}O vs δ ^{2}H) of atmospheric moisture.

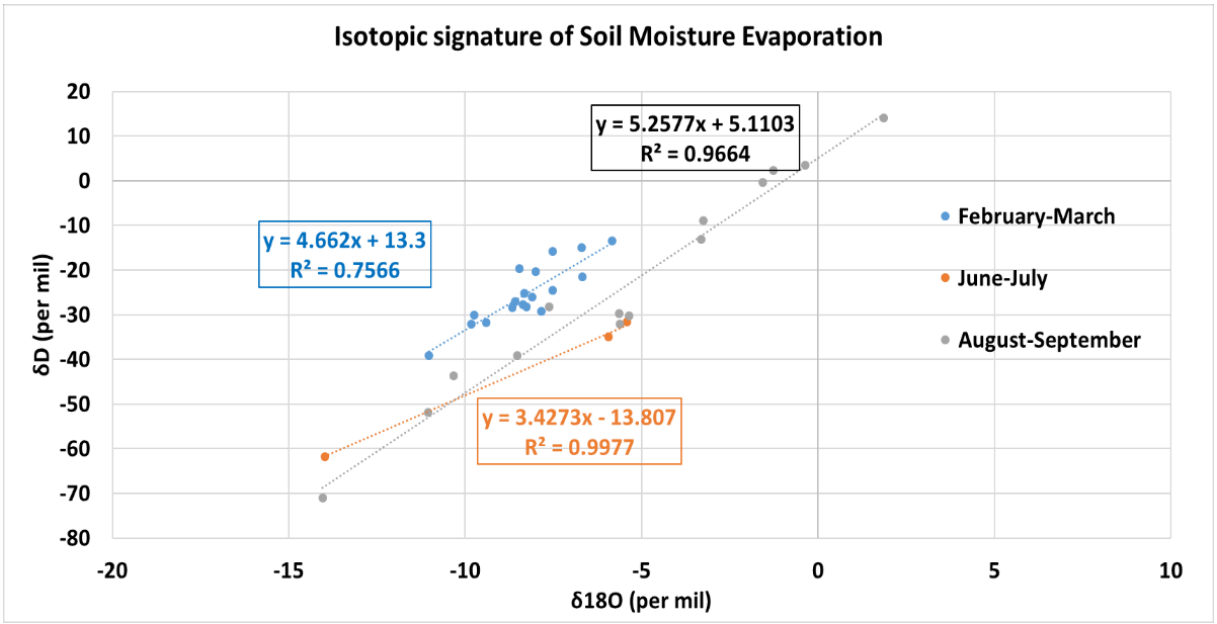

Figure A22: Seasonal variations of isotopic signature (δ 18O vs δ 2H) of soil evaporation.

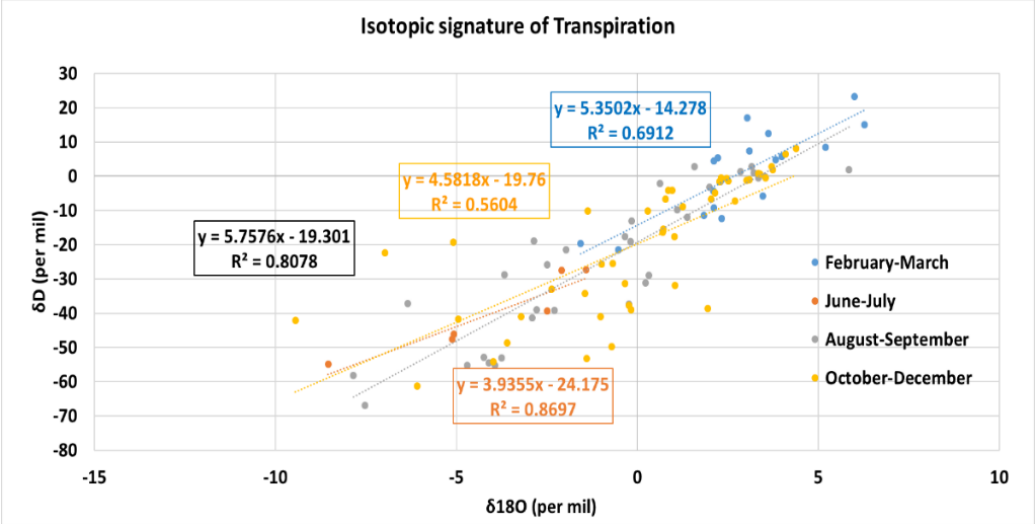

Figure A23: Seasonal variations of isotopic signature (δ 18O vs δ 2H) of transpired water.

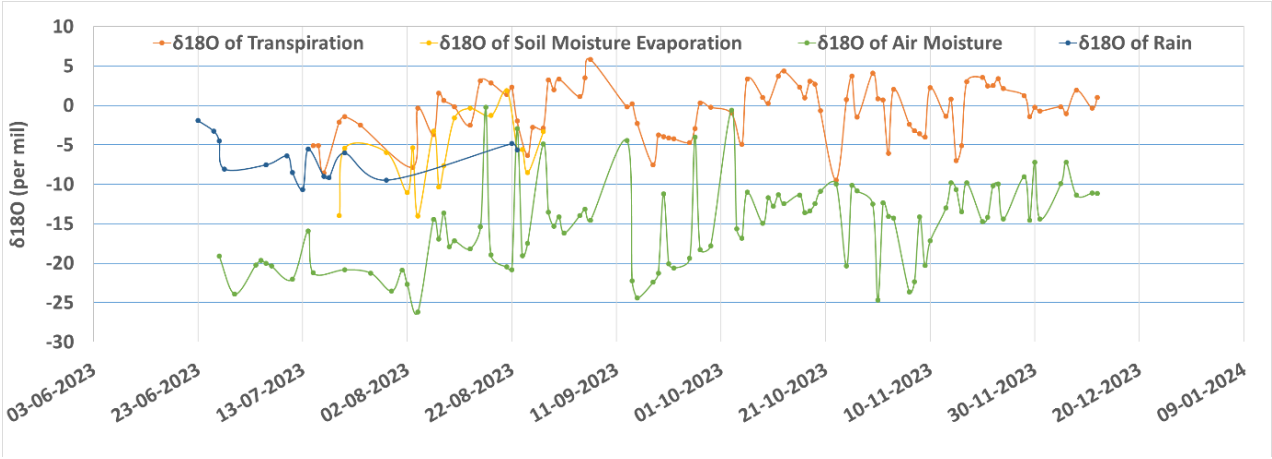

Figure A24: Temporal variation of the ^{18}O of transpiration, soil moisture, air moisture, evaporation and rain for 2023 measured at NIH Roorkee.

Publications

1. Singh et al. (2025). Evapotranspiration partitioning using stable isotopes of O and H, selected for poster presentation in *EGU 2025*.
2. Krishan et al. (2024). Partitioning of Evapotranspiration into Evaporation and Transpiration fluxes using Stable Water Isotopes and Temporal Change Detection in Isotopic Values with Atmospheric Temperature and Air Moisture Changes. In: *International conference on future of water resources*, January 18-20, 2024, at IIT and NIH, Roorkee.
3. Krishan et al. (2024). Intra-annual variations in isotopic composition of atmospheric water vapour in a semi-arid monsoon region: observations and inferences. Discover Atmosphere. 2, 7. https://doi.org/10.1007/s44292-024-00010-w
4. Singh et al. (2023). Development of Local Meteoric Water Line for Kanpur, Uttar Pradesh, In: 28th *International Conference on Hydraulics, Water Resources & Coastal Engineering, (HYDRO, 2023)*, December 20-22, 2023, at NIT Warangal. https://link.springer.com/chapter/10.1007/978-981-97-7467-8_3
5. Singh et al. (2022), Methodological considerations for the collection of air moisture for isotopic analysis, In: *Roorkee Water Conclave 2022*, IIT Roorkee
6. Singh et al. (2022), A Comparison of the Rain Gauges of Various Sizes and Measuring Principles, In: *27th International Conference on Hydraulics, Water Resources & Costal Engineering, (HYDRO, 2022)*, Chandigarh.
7. Singh et al. (2022), Experimental setup for partitioning evapotranspiration at plot and field scales, In: *Advances in Water Resources Planning and Management, (AWRPM, 2022)*, IIT Madras Poster presentation.
8. Krishan, G. et al (2022) Influence of changing isotopic conditions of atmospheric moisture, precipitation, and groundwater on the seasonal variations in the isotopic composition of transpiration, In: *International conference on Recent advances in water science and technology (ICRAWST 2022)* organized by Department of Civil Engineering, Sri Shakti Institute of Engineering and Technology, Coimbatore, Tamil Nadu, 7-9th December 2022.